Overlapping redox zones control arsenic pollution in Pleistocene multi-layer aquifers, the Po Plain (Italy)

Marco Rotiroti[1], Tullia Bonomi[1], Elisa Sacchi[2], John M. McArthur[3], Rasmus Jakobsen[4], Alessandra Sciarra[5], Giuseppe Etiope[6], Chiara Zanotti[1], Veronica Nava[1], Letizia Fumagalli[1] and Barbara Leoni[1]*

[1]Department of Earth and Environmental Sciences, University of Milano-Bicocca, Piazza della Scienza 1, 20126 Milan, Italy.

[2]Department of Earth and Environmental Sciences, University of Pavia, Via Ferrata 1, 27100 Pavia, Italy.

[3]Department of Earth Sciences, University College London, Gower Street, WC1E 6BT London, United Kingdom.

[4]Geological Survey of Denmark and Greenland, Øster Voldgade 10, 1350 Copenhagen, Denmark.

[5]Istituto Nazionale di Geofisica e Vulcanologia, Sezione Roma 1, Via di Vigna Murata 605, 00143 Rome, Italy.

[6]Istituto Nazionale di Geofisica e Vulcanologia, Sezione Roma 2, Via di Vigna Murata 605, 00143 Rome, Italy.

*corresponding author, email: marco.rotiroti@unimib.it, tel: +39 0264482882.

Science of the Total Environment 2020, https://doi.org/10.1016/j.scitotenv.2020.143646

Received 28 August 2020, Revised 26 October 2020, Accepted 3 November 2020, Available online 21 November 2020

For the full version go to https://www.sciencedirect.com/science/article/pii/S0048969720371771?via%3Dihub

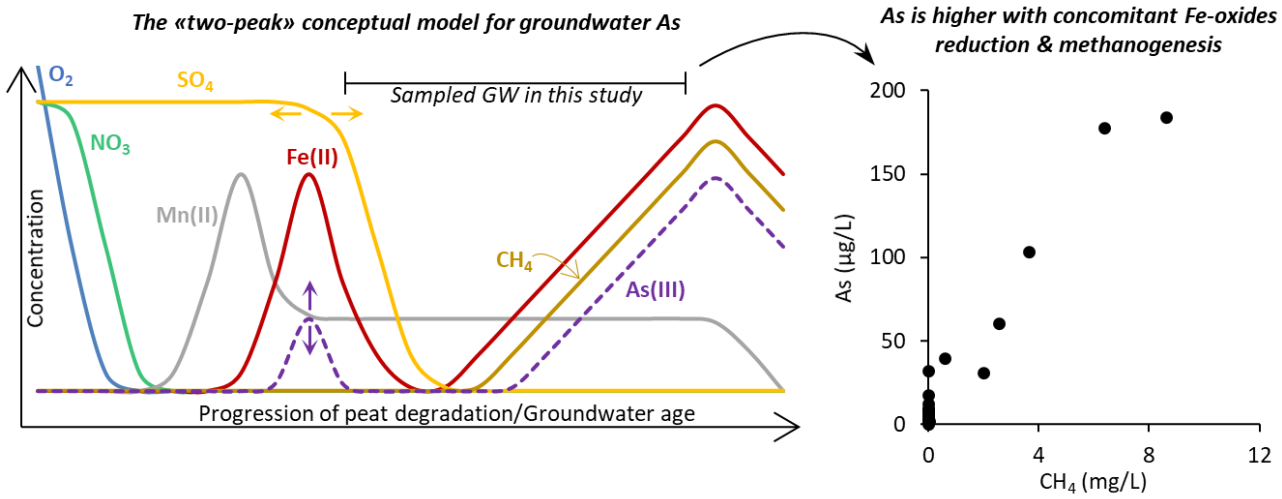

Abstract

Understanding the factors that control As concentrations in groundwater is vital for supplying safe groundwater in regions with As-polluted aquifers. Despite much research, mainly addressing Holocene aquifers hosting young (<100 yrs) groundwater, the source, transport, and fate of As in Pleistocene aquifers with fossil (>12,000 yrs) groundwaters are not yet fully understood and so are assessed here through an evaluation of the redox properties of the system in a type locality, the Po Plain (Italy).

Analyses of redox-sensitive species and major ions on 22 groundwater samples from the Pleistocene arsenic-affected aquifer in the Po Plain shows that groundwater concentrations of As are controlled by the simultaneous operation of several terminal electron accepters. Organic matter, present as peat, is abundant in the aquifer, allowing groundwater to reach a quasi-steady-state of highly reducing conditions close to thermodynamic equilibrium. In this system, simultaneous reduction of Fe-oxide and sulfate results in low concentrations of As (median 7 μg/L) whereas As reaches higher concentrations (median of 82 μg/L) during simultaneous methanogenesis and Fe-reduction. The position of well-screens is an additional controlling factor on groundwater As: short screens that overlap confining aquitards generate higher As concentrations than long screens placed away from them. A conceptual model for groundwater As, applicable worldwide in other Pleistocene aquifers with reducible Fe-oxides and abundant organic matter is proposed: As may have two concentration peaks, the first after prolonged Fe-oxide reduction and until sulfate reduction takes place, the second during simultaneous Fe-reduction and methanogenesis.

Keywords: Groundwater quality, TEAPs, peat, methanogenesis, sulfate, iron.

1. Introduction

Arsenic pollution of groundwater affects many areas around the world (Ravenscroft et al., 2009). South and South-East Asia are the most As-affected regions worldwide (Fendorf et al., 2010; McArthur, 2019), where over 100 million people are being exposed (Ravenscroft et al., 2009), with other regions being less affected. In Europe, groundwater in two large areas is affected by As pollution: a) the Pannonian Basin, covering 325,000 km^2 (Gyuró, 2007) between Hungary, Romania, Serbia, Slovakia and Croatia, with nearly 1 million people exposed to drinking waters with As greater than the WHO standard of 10 μg/L (Rowland et al., 2011); b) the Po Plain of Italy, which covers an area of 46,000 km^2 and is home to around 20 million inhabitants. In the Po Plain, groundwater for public consumption is treated to keep As <10 μg/L before it is distributed, so As in locally-grown food poses a greater risk

than does As in groundwater (Cubadda et al., 2010; Di Giuseppe et al., 2014), owing to the use of As-polluted water for irrigation. Nevertheless, the ability to tap As-free groundwater remains an important target for the managers of any drinking water supply, with a primary aim being to minimize the cost of water purification. Additionally, in the next years, the limit for As of 10 μg/L may be lowered, as it has been in Denmark (5 μg/L; Ersbøll et al., 2018) and may soon be in the Netherlands (1 μg/L; Ahmad et al., 2020). Moreover, following the approach of water safety planning (WSP) recommended by WHO (2011) and implemented by EC (2015) and Italian regulations (D. M. S. 14.06.17, 2017), drinking-water managers are required to adopt a preventive approach to mitigate the health risks from As posed to consumers. To this end, the quest for As-free groundwater is key. Although previous studies described the severity of As pollution in the Po Plain, and proposed conceptual models for interpreting As dynamics (Carraro et al., 2015; Cavalca et al., 2019; Giuliano, 1995; Molinari et al., 2013; Rotiroti et al., 2017, 2015; Zuzolo et al., 2020), an in-depth evaluation of the factors controlling the source, transport and fate of As in groundwater is still lacking.

Parallels can be drawn between the As-pollution of aquifers beneath the Po Plain and those in South and South-East Asia. In SE Asia, the reductive dissolution of Fe-oxide, driven by organic matter (OM) degradation, is the main mechanism for As release to groundwater (Nickson et al., 1998 et seq.). In SE Asia, As-pollution mostly affects shallow Holocene aquifers (mostly <50 m below ground surface; bgs), whereas deeper Pleistocene aquifers are mostly As-free (Ravenscroft et al., 2009). The difference is attributed to the fact that OM is more abundant in the shallow Holocene aquifers (Ravenscroft et al., 2009; Sutton et al., 2009). The severity of the problem of As-pollution in SE Asia has attracted much research effort focused on Holocene aquifers with young (<100 yrs) groundwaters (Radloff et al., 2017; Richards et al., 2019; Sø et al., 2018), whereas Pleistocene aquifers hosting fossil (>12,000 yrs) groundwater, as the case of the Po Plain (Martinelli et al., 2014; Zuppi and Sacchi, 2004), are much less explored.

The aim of the present work is to identify the main controls on groundwater As in the deep pre-Holocene aquifers, with the aquifers of the Po Plain being an exemplar, in order to aid prediction of where low-As groundwater can be found in such aquifer, thereby supporting the management of such groundwater resources. To accomplish our aims, new hydrochemical field data, including dissolved CH_4 and H_2, was collected from wells used for irrigation, livestock farming, and public water-supply. The data is used to improve the existing conceptual model for As mobilization in the Po Plain, a model that invokes the reductive dissolution of Fe-oxides driven by the degradation of peat-derived OM.

2. Materials and Methods

2.1. Study Area

The study area encompasses ~500 km^2 of the lower Po Plain of North Italy (Fig. S1). This area is the southern portion of a larger area previously studied through 5 field surveys (Sect. 2.2; Rotiroti et al., 2019a, 2019b; Zanotti et al., 2019) that provided a detailed description of the hydrology, hydrogeology and hydrochemistry of the study area: a brief summary is given here. The alluvial sediments of the Po Plain are Pleistocene in age, except for the shallower part (<30-40 m bgs) of the river valleys (Fig. S1) that are filled with Holocene sediments (Marchetti, 2002). Alternating silts/clays and sands (Fig. S1), form a multi-layer stacked aquifer system (Giuliano, 1995; Ori, 1993; Perego et al., 2014). Silt and clay aquitards often contain buried peats (Amorosi et al., 2008; Miola et al., 2006). The aquifers are confined, except where the confining layer thins locally to create semi-confined or unconfined conditions. Groundwater flow in the deeper system (>40 m bgs) is from NW to SE (Fig. S1). In the shallow parts of the system (<40 m bgs), baseflow to local, gaining, rivers imparts strong local variations to the direction of groundwater flow (Rotiroti et al., 2019a). Groundwater recharge is mainly from inflow sourced by upstream areas, as the widespread presence of shallow confining clays and silts prevents or restricts infiltration from surface sources. Locally, however, patchy coarser sediments allow some local recharge by returning irrigation water or infiltration from irrigation channels. In addition, a pumping-induced recharge from rivers or irrigation channels occurs where wells are sited close to surface water bodies (Rotiroti et al., 2019a).

Groundwater tracers enabled Rotiroti et al. (2019a) to classify groundwater samples into two groups: a) older groundwaters with little or no local recharge (Cl/Br <340 and δ^2H >−60‰); and b) younger groundwaters (Cl/Br >340 and δ^2H <−60‰) whose composition approach the values in the Oglio River ($\delta^2H \approx -65$‰ and Cl/Br between 474 and 733). Groundwaters are reducing and of the Ca-HCO_3 type, with low Cl content (median concentration of 3.0 mg/L; Rotiroti et al., 2019a).

2.2. Groundwater sampling and analysis

Groundwater samples were collected in July 2017 from 22 wells (Fig. S1). The wells targeted were those for which complete information was available (well and screen depths, lithology). Most had only one screen, but 2 had two screens and 3 had five screens. Locations were chosen to obtain as regular a sample grid as possible and, where

possible, to provide a depth profile, using wells that were close together but had different screened intervals. These wells were sampled 5 times before (October 2015, February, June, September 2016 and March 2017) for the analysis of major ions, trace elements (As, Fe and Mn) and water isotopes; the results were reported in Rotiroti et al. (2019a, 2019b). The present study extends the range of parameters measured in those studies, comprising pH, electrical conductivity (EC), oxidation-reduction potential (ORP), dissolved O_2 (DO), water temperature, alkalinity, chloride (Cl), nitrate (NO_3), sulfate (SO_4), ammonium (NH_4), calcium (Ca), magnesium (Mg), sodium (Na), potassium (K), total arsenic (As), As(III), As(V), iron (Fe), manganese (Mn), total phosphorous (P-tot), dissolved organic carbon (DOC), methane (CH_4), dihydrogen (H_2), water isotopes ($\delta^{18}O/\delta^{2}H$ in H_2O), carbon isotopes ($\delta^{13}C$) in CH_4 (only for 9 samples) and nitrogen isotopes ($\delta^{15}N$) in NH_4 (only for 8 samples collected in September 2016). In addition, measures of the ratio between chloride and bromide (Cl/Br) were available from the previous sampling surveys in June and September 2016 (Rotiroti et al., 2019a). Details of sampling methods, field measurements and laboratory analyses are reported in Sup. Info. Sect. S3 together with limits of detection (LOD) and analytical uncertainties (Table S1). Charge-balance error (CBE) was used as a means for evaluating analytical techniques (Fritz, 1994). The average (mean ± standard deviation) CBE was 0.65 ± 0.70 % and 0.83 ± 0.47 % in terms of absolute values, below the recommended threshold of 2% (Fritz, 1994). Calculation of speciation and saturation indices (SI's) was done using PHREEQC (Parkhurst and Appelo, 2013) and the wateq4f database (Ball and Nordstrom, 1991). Speciation was computed using pe values derived from field ORP measurements ($E_{Ag/AgCl}$). Energetics of terminal electron accepting processes (TEAPs) was assessed by calculating the Gibbs free energy of reaction at system condition using PHREEQC, considering the activities computed during speciation. Reduction half-reactions, with H_2 as electron donor, were considered in this calculation because the H_2 level reflects the internal redox state of many different anaerobic microorganisms, regardless of the main electron donor (Hoehler et al., 2001). Details on stoichiometry are given in Table S2. Since sulfides were not measured in this study, the activity of HS^- was calculated by assuming equilibrium with FeS.

3. Results and Discussion

3.1. Peat degradation governs groundwater chemistry

Sampled groundwater is reducing and contains <0.2 mg/L of DO and NO_3. Italian regulatory limits of 10, 200, 50 and 500 µg/L for As, Fe, Mn and NH_4 are exceeded, respectively, in 9, 14, 20 and 14 of our 22 well waters (Table S1, Fig. S2). These reducing conditions are generated by the degradation of OM in localized deposits of peat within the

clay and silt aquitards. The widespread distribution of peat over the entire depth-range studied (up to 200 m bgs) is confirmed by its recorded presence in numerous lithologs (Bonomi et al., 2014; Rotiroti et al., 2019a) and by other reports of its presence in cores drilled in the lower Po Plain (Carraro et al., 2015; Miola et al., 2006; Rotiroti et al., 2014; Sciarra et al., 2013; Zuppi and Sacchi, 2004). The peats were formed in abandoned meanders and zones of water stagnation generated by river avulsion and subsequently buried by younger alluvium (Miola et al., 2006). Microbial metabolism of sedimentary OM generates organic molecules, ammonium, and phosphate, which are released to groundwater along with Br (Gerritse and George, 1988). Although typically treated as conservative in groundwater, the Cl/Br of unpolluted groundwater may decline as OM degradation releases more Br than Cl. Ammonium can have a conservative behavior under strong reducing conditions, although it can be removed from groundwater by cation exchange: a consequence of ion-exchange is to lessen the concentration even where a steady supply of NH_4 is available *via* organic degradation. Our recorded concentrations of NH_4 are therefore not an indication of total OM mineralization. Nevertheless, increasing DOC and NH_4, and decreasing Cl/Br values, trace the progression of OM degradation (Böhlke et al., 2006; Desbarats et al., 2014). The strong positive correlation of DOC with NH_4 and P-tot (Pearson correlation coefficient r of 0.98 and 0.95 with p-values of $6.5e^{-16}$ and $4.5e^{-13}$, respectively; Table S3) and the negative correlation of Cl/Br with DOC (r of −0.74 with p-value of $3.8e^{-5}$; Table S3), and thus with NH_4 and P-tot, found in our data (Fig. 1) indicate that the studied system is experiencing OM degradation with an accumulation of by-products.

Based on predominant TEAPs, the sampled groundwaters may be grouped into three classes (Fig. 1); these are: 1) Fe-oxide reduction and early-stage sulfate reduction for samples with SO_4 >10 mg/L; 2) Fe-oxide reduction and advanced-stage sulfate reduction with SO_4 <10 mg/L and CH_4 <0.5 mg/L; 3) Fe-oxide reduction and methanogenesis with SO_4 <1.5 mg/L and CH_4 >0.5 mg/L. The expected succession through the classes, the clean transition between them seen in our data, and the accompanying increasing DOC and NH_4 and decreasing Cl/Br, all confirm that there is a progressing degradation of OM within the system. This evidence of degradation, together with the fact that this redox classification was based on Fe, SO_4 and CH_4 rather than on DOC, NH_4 and Cl/Br, validates our classification. Fe-oxide reduction is considered to occur in all these three classes due to the presence of dissolved Fe (median concentration for all samples of 274 μg/L) and the considerations discussed in depth in Sect. 3.2. Concerning P-tot, its strong positive correlation with DOC is probably a result of the release of P from degrading OM. Additionally, the reductive dissolution of Fe-oxides, on which P is likely adsorbed (Ravenscroft et al., 2001), gives an extra input of P-tot to groundwater. Since Fe-oxides reduction proceeds together with OM degradation, the contribution from the two sources cannot be separated.

Microbial degradation of peat is also the likely source of dissolved CH_4 in groundwater, as suggested by the positive correlation between DOC and CH_4 (*r* of 0.90 with p-value of $1.9e^{-9}$; Table S3; data plotted in Fig. 1) and $\delta^{13}C_{CH4}$ values (from −75.2 to −62.4‰) that fall within the range of microbial methane (Mattavelli and Novelli, 1988; Milkov and Etiope, 2018). More specifically, the $\delta^{13}C$ values in four wells (LL50 and LR59-61) are <−70‰ (Table S1) indicating a source *via* CO_2 reduction (Milkov and Etiope, 2018; Whiticar, 1999), as in other aquifers worldwide (Aravena et al., 1995; Coleman et al., 1988; Hansen et al., 2001; Postma et al., 2012). In another five wells, $\delta^{13}C$ >−70‰, indicating a source *via* acetate fermentation. Furthermore, values of $\delta^{15}N_{NH4}$ ranging from 1.3 to 16.0‰ confirm that NH_4 is the product of local degradation of peat (see Sup. Info. Sect. S4). Finally, some thrust systems, which could facilitate the seepage of deep gas, are located within or close to the study area (Lindquist, 1999; Maesano and D'Ambrogi, 2016; Mattavelli et al., 1983; Rossi et al., 2015). Whilst we cannot exclude the possibility that such seepage contributes to our measured concentrations of CH_4, the good correlation between CH_4 and DOC suggests that such an influence is not present.

The degradation of OM is a strong influence on alkalinity and EC, and generates a positive correlation between DOC and, for example, Na and Ca (see Sup. Info. Sect. S5 for further details). The strong correlation of alkalinity with DOC (Fig. 1) and NH_4 (*r* of 0.84 and 0.85 with p-values of $3.6e^{-7}$ and $1.5e^{-7}$, respectively; Table S3) is the likely effect of dissolved inorganic carbon (DIC) production due to the mineralization of sedimentary OM, both as direct oxidation of organic to inorganic carbon and dissolution of carbonate minerals in response to the increase of acidity generated by the fermentation of OM (producing CO_2 and organic acids) during its degradation (Buckau et al., 2000). Speciation and calculation of SI's revealed that the role of buffering the increase in acidity is here likely played by the dissolution of rhodochrosite ($MnCO_3$), for which the groundwater was found to be near equilibrium, whereas a strong supersaturation was seen for calcite ($CaCO_3$), dolomite ($MgCa(CO_3)_2$) and siderite ($FeCO_3$; see Sup. Info. Sect. S6 for further details). The strong correlation of EC with DOC (Fig. 1) and NH_4 (*r* of 0.81 and 0.83 with p-values of $1.9e^{-6}$ and $4.3e^{-7}$, respectively; Table S3), that are all products or effects of OM degradation, indicates that groundwater salinity is mainly due to OM degradation. The low Cl concentrations in our groundwaters confirm that anthropogenic influences are insignificant in all but three wells (LL39, LL41, LR58) that contain between 19 and 34 mg/L of SO_4 and have Cl/Br >400. These three contain a vestigial anthropogenic influence inherited from upstream recharge areas or a more recent anthropogenic influence conveyed by the component of younger recharge attributable to these wells (Table S1). However, higher $\delta^{18}O$ and $\delta^{2}H$ values with increasing EC indicate that younger, human-impacted, recharge from the surface, having more depleted isotope values (Rotiroti et al., 2019a), does not contribute significantly to the EC. This

confirms that the main source of OM is buried peat, indicating that a possible infiltration of OM from the surface, either of anthropogenic (e.g. sewage, manure) or natural (e.g. riverine) origin, is unlikely or minor.

3.2. Different TEAPs occur simultaneously: overlapping redox zones

Traditionally, the sequence of TEAPs accompanying OM oxidation follow a hierarchy of decreasing Gibbs free energy (Champ et al., 1979; Lovley and Goodwin, 1988; McMahon and Chapelle, 2008). This linear succession of redox reactions and zones implies that competitive exclusion exists within bacteria communities that mediate successive redox zones (Chapelle and Lovley, 1992). It is clear from our data, however, that for the least energetically favored TEAPs, the conventional fixed hierarchical sequence does not apply in groundwaters at circumneutral pH. Instead, Fe-oxide reduction, sulfate reduction and methanogenesis can proceed either in a different order or simultaneously, as suggested for groundwater elsewhere (Bethke et al., 2011; Postma and Jakobsen, 1996). The reasons for this different order are several. Firstly, Fe-oxide reduction is pH-dependent and, at circumneutral pH, the reduction of more stable Fe-oxides (e.g. magnetite, goethite) is energetically unfavorable (lower release of Gibbs free energy) with respect to methanogenesis and sulfate reduction (Bethke et al., 2011). Secondly, considering usable, rather than available, energy (the difference between the available energy and that maintained by bacteria to sustain their life functions; Jin and Bethke, 2009, 2003), Fe-oxide reduction, sulfate reduction and methanogenesis provide approximately the same amounts of energy at near neutral pH in groundwater (Bethke et al., 2011). Thus, energetics cannot establish a fixed order for the progression of late stage redox reactions. Thirdly, microbial ecology suggests that mutualistic, rather than competitive, relationships between bacteria may mediate the use of TEAPs, so the simultaneous use of two TEAPs might be favored; for example, by the removal by precipitation of their by-products, as postulated for the simultaneous operation of Fe-oxide reduction and sulfate reduction aided by precipitation of iron sulfide (Bethke et al., 2011; Postma and Jakobsen, 1996), and simultaneous Fe-oxide reduction and methanogenesis with precipitation of siderite (Jakobsen and Cold, 2007).

Although microbial ecology and kinetic limitations play a role, together with microbial microenvironments (Murphy et al., 1992), in which favorable conditions for specific TEAPs can develop locally on a micro scale (e.g. the increase in acidity in a biofilm surrounding a fragment of fermenting OM can favor local goethite reduction; Bethke et al., 2011) an aquifer system with a high supply of OM developing strong reducing conditions (where Fe-oxide reduction, sulfate reduction and methanogenesis can take place) can be well-described, on the whole, by equilibrium thermodynamics (Bethke et al., 2011), according to the partial equilibrium approach (Postma and Jakobsen, 1996). This

considers the OM degradation as a two-steps process (Lovely, 1987): 1) the hydrolyzation and fermentation of OM with the production of simpler compounds as formic acid, acetic acid, H_2 and CO_2; this is the rate-determining step; 2) the consumption of the fermentative products by different TEAPs; this step is assumed to approach equilibrium. However, full equilibrium is not obtained as a small amount of energy is used for growth by the microorganisms mediating the processes. The partial equilibrium approach is applicable for Mn-oxide, Fe-oxide and sulfate reduction and methanogenesis, but it is not adequate for DO reduction and denitrification since they involve a direct OM metabolization by bacteria (Appelo and Postma, 2005).

Our sampled groundwaters are in redox states where the electron acceptors for DO reduction, denitrification and Mn-oxide reduction have been exhausted (DO and NO_3 <0.2 mg/L and mean Mn = 110 µg/L), so Fe-oxide reduction, sulfate reduction and methanogenesis either occur successively as the predominant TEAP (in the classical view) or occur simultaneously. In our system, the simultaneous occurrence of Fe-oxide and sulfate reduction, together with the precipitation of their products as iron sulfides, is supported by the plot of Fig. 2a, showing that many samples are aligned along a slope similar to the equilibrium lines of simultaneous Fe-oxide reduction, sulfate reduction and FeS precipitation (the stoichiometry and the equilibrium equation are given in Table S4). Moreover, many groundwaters fit a modelled equilibrium involving a hypothetical Fe-oxide (solubility product for which logK is 0.78; Rotiroti et al., 2015) that is in the range of stability of goethite and lepidocrocite (Cornell and Schwertmann, 2003). This phase may be considered as a theoretical, moderately stable, Fe-oxide, representing the average of a mixture of low and high stability oxides likely present in the aquifer, for which the overall system approaches a thermodynamic equilibrium. The fact that the composition of three groundwaters that are classified as Fe-oxide reduction and methanogenesis (wells LR59-61) align with this equilibrium line could indicate that sulfate reduction may still be ongoing, likely at slow rates, even where methanogenesis is predominant. Alternatively, the simultaneous operation of Fe-oxide reduction, sulfate reduction and methanogenesis could be apparent, being, actually, the effect of mixing along well screens of groundwaters coming from different zones and having different conditions.

Notwithstanding the above, three other groundwaters that are classed as Fe-oxide reduction and methanogenesis (wells LL47, LL50 and OV77) depart more from equilibrium, likely indicating that, in these groundwaters, sulfate reduction is not occurring, but that methanogenesis occurs simultaneously with Fe-oxide reduction. This interpretation is supported by a) the proximity of these three samples (wells LL47, LL50 and OV77) to the equilibrium line of simultaneous Fe-oxide reduction and methanogenesis (Fig. 2a; see Table S4 for stoichiometry and equilibrium equation) and b) the positive correlation of Fe with DOC and CH_4 (Fig. S3) for groundwaters with Fe-oxide reduction and methanogenesis. Fe-oxide reduction and methanogenesis were previously reported to occur

concomitantly near equilibrium in reducing groundwaters worldwide (Jakobsen and Cold, 2007; Postma et al., 2007; Zhou et al., 2014) and simulated through modelling (Jakobsen, 2007; Rotiroti et al., 2018). Their simultaneous occurrence could be the result of a mutualistic relationship between Fe-reducing bacteria and methanogens aided by the precipitation of siderite (Jakobsen and Cold, 2007). However, siderite precipitation often occurs far from equilibrium (i.e. at supersaturation; Postma, 1982) due to a kinetic inhibition exerted by OM and PO_4 (Berner et al., 1978). Kinetic inhibition seems confirmed in our system by the supersaturation seen for siderite and the correlation between its SI and DOC (Sup. Info. Sect. S6).

Additional evidence of the presence of overlapping redox zone in our groundwaters can be obtained from a further consideration of energetics. Fig. 2b shows computed values of Gibbs free energy of reaction at our system conditions (ΔG_r) for Fe-oxide reduction (considering the various oxides at different stabilities listed in Table S2), sulfate reduction and methanogenesis, compared to a range of threshold energy values (ΔG_{min}; representing the energy level maintained by the microbes) taken from literature (Hoehler, 2004; Jakobsen and Cold, 2007; Rotiroti et al., 2018), so that an estimation of the usable energy ($\Delta G_r - \Delta G_{min}$) can be given. The usable energy for all the three TEAPs (considering the hypothetical medium-stable oxide for Fe-reduction) results in the order of a few kJ/mol per H_2 (Fig. 2b), confirming the findings by Bethke et al. (2011) of roughly equivalent amounts. Fe-oxide reduction is more favorable ($\Delta G_r < \Delta G_{min}$) for relatively unstable oxides, such as lepidocrocite and ferrihydrite (not shown), and unfavorable ($\Delta G_r > \Delta G_{min}$) for relatively stable oxide, such as goethite and hematite (not shown). The reduction of the hypothetical middle-stability oxide (representing average system-conditions), for which most of the samples align in the plot of Fig. 2a, has an available energy, for all samples, in the range of the threshold energy ($\Delta G_r \approx \Delta G_{min}$), giving a usable energy close to zero. An energy close to zero thus confirms that Fe-oxide reduction may occur close to a thermodynamic equilibrium in all the three classes of samples identified here. A similar condition (i.e. $\Delta G_r \approx \Delta G_{min}$) is found for sulfate reduction in samples classified as 'Fe-oxide reduction and advanced-stage sulfate reduction' and for methanogenesis in samples classified as 'Fe-oxide reduction and methanogenesis'. The usable energy close to zero for a) Fe-oxides reduction and b) sulfate reduction or methanogenesis in specific samples confirms the presence in our samples of a "partial" equilibrium state in which simultaneous Fe-oxide reduction/sulfate reduction or Fe-oxide reduction/methanogenesis can occur, respectively.

Finally, some considerations must be given to Mn-oxide reduction. The assertation made above that Mn-oxide reduction is complete in our groundwaters is supported by Fig. S4, in which samples plot far from, and with a different slope to, the equilibrium line for Mn-oxide reduction. This departure from equilibrium precludes equilibrium with other TEAPs. We propose that Mn-oxide reduction occurred upflow in the aquifer in earlier stages of OM degradation and so

has not been captured by our samples as the product of Mn-reduction. Rather, we propose that dissolved Mn in our groundwaters, produced upflow, is now controlled by the dissolution/precipitation equilibrium of rhodochrosite. This equilibrium, together with the likely role played by rhodochrosite in buffering acidity, as discussed in Sect. 3.1, implies that high Mn concentrations are maintained by rhodochrosite dissolution. Such a proposal agrees with the fact that selective sequential extractions of aquifer sediments from the Po Plain showed that Mn is mostly present in the sediment as carbonate (Molinari et al., 2014).

3.3. What controls groundwater As?

The positive correlation of As with DOC, NH_4 and P-tot (r of 0.87, 0.89 and 0.90 with p-values of $3.6e^{-8}$, $7.7e^{-9}$ and $3.1e^{-9}$, respectively; Table S3) and its negative correlation with Cl/Br (r of −0.65 with p-value of $6.1e^{-4}$; Table S3; data plotted in Fig. 3) confirm that the degradation of peat is the driver of As release to groundwater in the Po Plain. Although As and Fe concentrations are frequently reported to have a poor correlation (see Ravenscroft et al., 2009 for reviews) because Fe is not conservative in solution, they show a covariation in our system, albeit weak, for groundwaters under methanogenesis (Fig. 3), confirming that Fe-oxide is the source of As release. Furthermore, the fact that dissolved As is present predominantly as As(III) in our groundwaters (Table S1) corroborates our view that reductive dissolution of Fe-oxide, driven by peat degradation, causes As-pollution of our groundwaters. However, the strong correlation of As with the products of OM degradation (Fig. 3), such as DOC, NH_4 and CH_4 (r of 0.97 with p-value of $8.9e^{-15}$; Table S3), can also indicate that As can also be released directly by peat degradation. During its formation and evolution, peat can sequestrate As by forming covalent bonds between dissolved As and its sulfur groups (Anawar et al., 2003; Eberle et al., 2020; Langner et al., 2012;), so the prolonged degradation of peat can be a direct source of As to groundwater. The content of As on OM in solid aquitard samples from the Po Plain was reported by Molinari et al. (2015) to be between 13.1 and 26.0% of total As in the solid matrix, the larger fraction (41 to 84%) being found in Fe and Mn oxyhydroxides and crystalline oxides, so aquitard OM represents a relevant potential source of As to groundwater in this system.

The mutual exclusion of As and SO_4 (Fig. 3) indicates that sulfate reduction, occurring together with Fe-oxide reduction, leads to As sequestration *via* co-precipitation in FeS, formed by the products of these two reduction reactions, and/or via direct precipitation of As-sulfides (O'Day et al., 2004). The strong positive correlation between As and CH_4 (Fig. 3) is interpreted to be the result of the cessation of As sequestration by iron sulfides produced during sulfate reduction. Methanogenesis takes place after sulfate reduction is completed, as testified by the mutual exclusion

between CH_4 and SO_4 (Fig. S5), so the appearance of CH_4 marks the end of the As sequestration into precipitating sulfides. Therefore, during methanogenesis and Fe-reduction, As is released (from both reductive dissolution and peat degradation) with no or little attenuation processes, reaching the highest concentrations found in the groundwater.

The conclusion that As is high in groundwater during methanogenesis and Fe-reduction is confirmed by the interpretation of H_2 data, which are plotted against DOC and As in Fig. S6. Concentrations of As are low in groundwaters when simultaneous reduction of both Fe-oxide and sulfate occurs and also H_2 concentrations are between 1 and 4 nM, values that indicate active sulfate reduction (Chapelle et al., 1995). Concentrations of As are higher in groundwaters where both Fe-oxide reduction and methanogenesis occur together and concentrations of H_2 are between 2.7 and 4.7 nM. Although H_2 concentrations in both cases are below 5 nM, the minimum threshold proposed for methanogenesis by Chapelle et al. (1995), they are in the range 2–5 nM reported by Kirk et al. (2004) for groundwaters in which maximal concentrations of As occurred where both Fe-oxide reduction and methanogenesis was occurring simultaneously. Hansen et al. (2001) and Jakobsen and Cold (2007) also report the occurrence of methanogenesis together with Fe-oxide reduction when concentrations of H_2 are below 5 nM.

Concentrations of As in well water also may depend on the proximity of the screened interval(s) to organic-rich aquitards from which OM degradation by-products may be supplied by aquitard diffusion (McMahon and Chapelle, 1991). Wells screened proximally to aquitards have higher concentrations of As than do wells screened distally (Erickson and Barnes, 2005; Meliker et al., 2008). Longer screens, having a higher proportion of distal screen, also have lower As concentrations than do short screens where all the screen may be close to an aquitard (Erickson and Barnes, 2005; Meliker et al., 2008). For our wells, the linear or near-linear relations shown in Fig. 1 and 3, for samples characterized by Fe-oxide reduction and methanogenesis, may indicate that the position of the screens with respect to aquitards is also affecting As concentrations in our wells. The highest As value (184 µg/L) was measured in well OV77 which has 2 m (out of 9.5 m) of screen juxtaposed to a clay interval, whereas the lowest As for samples characterized by Fe-oxide reduction and methanogenesis (40 µg/L) was found in well LR60 in which no part of the 15 m screen was juxtaposed to a clay aquitard and the screen is 1.5 m distant from the aquitard (we discount well LL47 with 31 µg/L of As because we have no information on lithology or screen interval). In well LR59, which has 104 µg/L of As in its water, an intermediate condition is found: a screen 4 m long is placed adjacent to a confining clay. These observations support the hypothesis that the position of well screens can influence As concentrations in abstracted groundwaters.

3.4. The "two-peaks" conceptual model for groundwater As

Fig. 4 schematizes, for the aquifer systems of the Po Plain, how the concentrations of As and other redox species evolve during ongoing degradation of peat: the figure is based both on our data and the work of others (e.g. Appelo and Postma, 2005; Berner, 1981; Kirk et al., 2004; McArthur et al., 2004; Rotiroti et al., 2014; Sracek et al., 2018). In a system dominated by piston flow (i.e. with no mixing of groundwaters), the accumulated effect of the peat degradation is a function of time and so related to groundwater age; composition reflects an integration of all upstream reactions with those occurring in the present. At early stages of Fe-oxide reduction, and during Mn-oxide reduction, groundwater As is low due to its re-sorption onto residual oxides (Welch et al. 2000; McArthur et al., 2004). With the progression of Fe-oxide reduction, empty sorption sites on residual Fe-oxides decrease and dissolved As increases generating a first peak in As concentration. With the occurrence of sulfate reduction, dissolved As is attenuated by co-precipitation in FeS and/or precipitation in As-sulfides, such as realgar or orpiment (Carraro et al., 2015). The degree of attenuation depends on the amount of sulfate present and the proportion that is reduced. The degree of attenuation also depends on the degree of overlap between Fe-oxide reduction and sulfate reduction, which in turn is governed by the stability of Fe-oxides, pH and microbial ecology. Once sulfate reduction is complete, and methanogenesis occurs together with Fe-oxide reduction, dissolved As increases again. For this second peak in As concentration there will be little attenuation because most reactive Fe-oxides with large surface areas (i.e. sorption sites) have been reduced. The second peak concentration may exceed that of the first peak because of the possible derivation of some As directly from the OM itself. Dissolved As might increase until OM is completely mineralized or the system runs out of reducible Fe-oxide. After this point, dissolved As may decrease due to no new release and the attenuation of already released As. This could explain the decrease of As that is frequently found in the Po Plain aquifers at depth around and below 200 m bgs (Carraro et al., 2015; Rotiroti et al., 2014), where groundwaters can have ages up to ~50 kyrs (Martinelli et al., 2014; Zuppi and Sacchi, 2004). The attenuation must be assisted by a) dispersion, b) diffusion, c) flushing, albeit probably weak since groundwater at these depths have a sluggish circulation (hydraulic gradient around 0.1%; Rotiroti et al., 2019a) and d) adsorption onto siderite (Burnol and Charlet, 2010; Kocar et al., 2014) or other minerals. The last could be facilitated after the system has experienced prolonged and simultaneous Fe-oxide reduction and methanogenesis, a condition that may be favored by siderite precipitation (Sect. 3.2).

This conceptual model is based on the assumption of a widespread presence of reducible Fe-oxides and buried peat in the system, the latter ensures a large stock of OM, providing a constant OM input to the aquifer, a condition that seems to be valid in the study area and in the entire lower Po Plain (Carraro et al., 2015; Rotiroti et al., 2015; Sciarra et

al., 2013), although our DOC levels did not reach high levels, as reported in other OM-rich aquifers worldwide (Buckau et al., 2000).

The application of our conceptual model helps to interpret the variability of As in space and over depth in the study area. There is no relation between depth and redox states (Fig. S7), and thus, according to the conceptual model, between depth and As. For instance, methanogenesis takes place both at shallower and deeper depths, therefore high As values can be found both in shallow (e.g. well LR59) and deep (e.g. well OV77) groundwaters. Based on our data analyses, this means that groundwaters at the same depth can have different ages. Groundwater ages are related to geographical location, determining the length of groundwater flowpaths: wells located in the north-western part of the study area, upstream with respect to groundwater flow (Fig. S1), have shorter flowpaths, younger groundwater ages and higher redox states, whereas those located downstream in the south-eastern zone (Fig. S1), have longer flowpath, older ages and lower redox states. In addition to this, wells with a component of younger recharge, due to pumping-induced recharge from nearby rivers or irrigation channels (Rotiroti et al., 2019a), have an average groundwater age that is younger than ages for water from more distal wells (e.g. wells LL51 and LR58; Fig. S1), so the redox states are higher and As accordingly lower. In other words, younger recharge from the surface, probably containing higher SO_4 (and NO_3), favors sulfate reduction (or denitrification, which is energetically favorable compared to Fe-oxide reduction) suppressing As release.

3.5. Worldwide implications

A brief comparison of main factors controlling As pollution in South and South-East Asia with those in the Po Plain is discussed below. Concerning the Holocene aquifers in SE Asia, concentrations of dissolved As decline as sediment age increases and OM reactivity decreases (Postma et al., 2012; Stuckey et al., 2016). An additional constrain on As concentration is groundwater residence time (Sø et al., 2018), which determines the time available for sediment/groundwater interaction, the number of pore volumes flushed through the aquifer system, and controls the removal of dissolved and desorbed reaction products. In Vietnam, the deeper Pleistocene aquifers contain >10 µg/L As only where extensive pumping has localized drawdown of As and/or OM from shallow, Holocene, aquifers (Winkel et al., 2011). In the Bengal Basin, As polluted groundwaters in the deep Pleistocene aquifer are found almost invariably in the absence of a palaeosol aquiclude that separates Holocene and Pleistocene aquifers across significant parts of the basin (McArthur et al., 2008, 2016), facilitating the downward transport of OM driving As release (McArthur, 2019) or

recharge of As-rich water from the Holocene as a result of groundwater pumping, although two instances of As-pollution by aquitard diffusion has been reported (Planer-Friedrich et al., 2012; Mihajlov et al., 2020).

Unlike South and South-East Asia where the availability of OM is limited in deeper Pleistocene aquifers (Ravenscroft et al., 2009; Sutton et al., 2009), the OM is not limited over depth in the Po Plain where peat deposits are found at depths up to ~250 m bgs (Rotiroti et al., 2014). This is a substantial difference between the two aquifer systems implying that different key factors are controlling As pollution. For instance, younger sediment age and higher OM reactivity seem to have no role in determining As pollution in the Po Plain aquifer system, since here severe As pollution can be found also in groundwater hosted by older sediments, e.g. well LR61 with 177 µg/L of As taps two sandy layers from 97 to 103 and from 151 to 153 m bgs that have an age ranging between 0.45 and 0.63 Myrs (Maesano and D'Ambrogi, 2016). The finding for the study area that As pollution is more severe where methanogenesis takes place once sulfate reduction is complete has been reported to occur in other aquifers that contain abundant OM, such as the Hetao Plain of China (Wang et al., 2015), the Pannonian Basin between Hungary and Romania (Rowland et al., 2011) and the Mahomet and Glasford aquifers in Illinois, USA (Kelly et al., 2005; Kirk et al., 2004). Therefore, it appears that the conceptual model discussed in the present study can be applied to As polluted aquifers worldwide that contain abundant OM, together with reducible Fe-oxides, that allow groundwater to reach a quasi-steady-state of highly reducing conditions (close to thermodynamic equilibrium) and so generate overlapping redox zones.

4. Conclusions

The key factors controlling As pollution in groundwater of the Po Plain, Italy, may apply in other Pleistocene aquifers with fossil groundwaters worldwide, they are summarized below:

- the abundant organic matter, present as peat, coupled to much reducible Fe-oxide, allows groundwater to reach a quasi-steady-state of highly reducing conditions close to thermodynamic equilibrium, enabling the simultaneous operation of different TEAPs in overlapping redox zones;
- the main factor controlling the concentration of As in groundwater is the accumulated effect of peat degradation as reflected in groundwater age: simultaneous Fe-oxide reduction and methanogenesis leads to high-As groundwaters, whereas simultaneous Fe-oxide and sulfate reduction leads to low-As groundwaters;

- the proximity of well-screens to organic-rich aquicludes influences As concentrations in abstracted groundwaters: As concentrations are higher where screens are proximal to organic-rich aquicludes and lower when the screens are distal to such units;
- a “two-peaks” conceptual model for groundwater As can be implemented for the Po Plain and other Pleistocene aquifers with similar sediment composition worldwide: a first peak in As concentration occurs after prolonged Fe-oxide reduction and is diminished by sulfate reduction. The peak of As concentration depends on the degree of overlap between Fe-oxide reduction and sulfate reduction; the greater the overlap, the lower the As peak may be, subject to initial SO_4 concentrations, the stability of Fe-oxides, pH and microbial ecology. A second peak of As is reached during simultaneous Fe-reduction and methanogenesis, during which process As is released with no or little attenuation, so it can reach the highest concentrations.

Funding

This work was supported by Fondazione Cariplo [grant number 2014-1282] and through the scientific collaboration no. 2018-CONV25-0024 between University of Milano-Bicocca and INGV.

Acknowledgements

We thank Acque Bresciane, Padania Acque, A2A Ciclo Idrico and all private owners for letting us to sample their wells. We are grateful to Gennaro A. Stefania, Sara Taviani and Martina Patelli of University of Milano-Bicocca for field work, Valentina Soler and Maria Tringali of University of Milano-Bicocca for major ions and trace elements analyses, Gabriele Tartari of CNR-IRSA (Verbania, Italy) for DOC analysis and Vittorio Barella and Enrico Allais of ISO4 (Torino, Italy) for water and ammonium isotope analyses.

References

Ahmad, A., van der Wens, P., Baken, K., de Waal, L., Bhattacharya, P., Stuyfzand, P., 2020. Arsenic reduction to <1 µg/L in Dutch drinking water. Environ. Int. 134, 105253. https://doi.org/10.1016/j.envint.2019.105253

Amorosi, A., Pavesi, M., Ricci Lucchi, M., Sarti, G., Piccin, A., 2008. Climatic signature of cyclic fluvial architecture from the Quaternary of the central Po Plain, Italy. Sediment. Geol. 209, 58–68. https://doi.org/10.1016/J.SEDGEO.2008.06.010

Anawar, H.M., Akai, J., Komaki, K., Terao, H., Yoshioka, T., Ishizuka, T., Safiullah, S., Kato, K., 2003. Geochemical occurrence of arsenic in groundwater of Bangladesh: sources and mobilization processes. J. Geochem. Explor. 77, 109–131. https://doi.org/10.1016/S0375-6742(02)00273-X

Appelo, C.A.J., Postma, D., 2005. Geochemistry, Groundwater and Pollution, second. ed. Balkema Publishers, Leiden.

Aravena, R., Wassenaar, L.I., Barker, J.F., 1995. Distribution and isotopic characterization of methane in a confined aquifer in southern Ontario, Canada. J. Hydrol. 173, 51–70. https://doi.org/10.1016/0022-1694(95)02721-Z

Ball, J.W., Nordstrom, D.K., 1991. User's manual for WATEQ4F, with revised thermodynamic data base and text cases for calculating speciation of major, trace, and redox elements in natural waters. U.S. Geological Survey Open-File Report 91–183. https://doi.org/10.3133/ofr91183

Berner, R.A., 1981. A new geochemical classification of sedimentary environments. J. Sediment. Res. 51, 359–365. https://doi.org/10.1306/212F7C7F-2B24-11D7-8648000102C1865D

Berner, R.A., Westrich, J.T., Graber, R., Smith, J., Martens, C.S., 1978. Inhibition of aragonite precipitation from supersaturated seawater; a laboratory and field study. Am. J. Sci. 278, 816–837. https://doi.org/10.2475/ajs.278.6.816

Bethke, C.M., Sanford, R.A., Kirk, M.F., Jin, Q., Flynn, T.M., 2011. The thermodynamic ladder in geomicrobiology. Am. J. Sci. 311, 183–210. https://doi.org/10.2475/03.2011.01

Böhlke, J.K., Smith, R.L., Miller, D.N., 2006. Ammonium transport and reaction in contaminated groundwater: Application of isotope tracers and isotope fractionation studies. Water Resour. Res. 42, W05411. https://doi.org/10.1029/2005WR004349

Bonomi, T., Fumagalli, L., Rotiroti, M., Bellani, A., Cavallin, A., 2014. The hydrogeological well database TANGRAM©: a tool for data processing to support groundwater assessment. Acq. Sott. Ital. J. Groundw. 3, 35–45. https://doi.org/10.7343/as-072-14-0098

Buckau, G., Artinger, R., Geyer, S., Wolf, M., Fritz, P., Kim, J.I., 2000. Groundwater in-situ generation of aquatic humic

and fulvic acids and the mineralization of sedimentary organic carbon. Appl. Geochem. 15, 819–832. https://doi.org/10.1016/S0883-2927(99)00078-5

Burnol, A., Charlet, L., 2010. Fe(II)−Fe(III)-Bearing Phases As a Mineralogical Control on the Heterogeneity of Arsenic in Southeast Asian Groundwater. Environ. Sci. Technol. 44, 7541–7547. https://doi.org/10.1021/es100280h

Carraro, A., Fabbri, P., Giaretta, A., Peruzzo, L., Tateo, F., Tellini, F., 2015. Effects of redox conditions on the control of arsenic mobility in shallow alluvial aquifers on the Venetian Plain (Italy). Sci. Total Environ. 532, 581–594. https://doi.org/10.1016/J.SCITOTENV.2015.06.003

Cavalca, L., Zecchin, S., Zaccheo, P., Abbas, B., Rotiroti, M., Bonomi, T., Muyzer, G., 2019. Exploring Biodiversity and Arsenic Metabolism of Microbiota Inhabiting Arsenic-Rich Groundwaters in Northern Italy. Front. Microbiol. 10, 1480. https://doi.org/10.3389/fmicb.2019.01480

Champ, D.R., Gulens, J., Jackson, R.E., 1979. Oxidation–reduction sequences in ground water flow systems. Can. J. Earth Sci. 16, 12–23. https://doi.org/10.1139/e79-002

Chapelle, F.H., Lovley, D.R., 1992. Competitive Exclusion of Sulfate Reduction by Fe(lll)-Reducing Bacteria: A Mechanism for Producing Discrete Zones of High-Iron Ground Water. Groundwater 30, 29–36. https://doi.org/10.1111/j.1745-6584.1992.tb00808.x

Chapelle, F.H., McMahon, P.B., Dubrovsky, N.M., Fujii, R.F., Oaksford, E.T., Vroblesky, D.A., 1995. Deducing the Distribution of Terminal Electron-Accepting Processes in Hydrologically Diverse Groundwater Systems. Water Resour. Res. 31, 359–371. https://doi.org/10.1029/94WR02525

Coleman, D.D., Liu, C.-L., Riley, K.M., 1988. Microbial methane in the shallow Paleozoic sediments and glacial deposits of Illinois, U.S.A. Chem. Geol. 71, 23–40. https://doi.org/10.1016/0009-2541(88)90103-9

Cornell, R.M., Schwertmann, U., 2003. The Iron Oxides: Structure, Properties, Reactions, Occurences and Uses, second. ed. Wiley-VCH, Weinheim. https://doi.org/10.1002/3527602097

Cubadda, F., Ciardullo, S., D'Amato, M., Raggi, A., Aureli, F., Carcea, M., 2010. Arsenic Contamination of the Environment−Food Chain: A Survey on Wheat as a Test Plant To Investigate Phytoavailable Arsenic in Italian Agricultural Soils and as a Source of Inorganic Arsenic in the Diet. J. Agric. Food Chem. 58, 10176–10183. https://doi.org/10.1021/jf102084p

Desbarats, A.J., Koenig, C.E.M., Pal, T., Mukherjee, P.K., Beckie, R.D., 2014. Groundwater flow dynamics and arsenic source characterization in an aquifer system of West Bengal, India. Water Resour. Res. 50, 4974–5002. https://doi.org/10.1002/2013WR014034

D. M. S. 14.06.17, 2017. Decreto del Ministero della Salute 14 giugno 2017 sul recepimento della direttiva (UE)

2015/1787 che modifica gli allegati II e III della direttiva 98/83/CE sulla qualita' delle acque destinate al consumo umano "Italian Ministerial Decree 14.06.17 on the implementation of Directive 2015/1787/EC amending Annexes II and III to Council Directive 98/83/EC on the quality of water intended for human consumption".

Di Giuseppe, D., Bianchini, G., Vittori Antisari, L., Martucci, A., Natali, C., Beccaluva, L., 2014. Geochemical characterization and biomonitoring of reclaimed soils in the Po River Delta (Northern Italy): implications for the agricultural activities. Environ. Monit. Assess. 186, 2925–2940. https://doi.org/10.1007/s10661-013-3590-8

Eberle, A., Besold, J., Kerl, C.F., Lezama-Pacheco, J.S., Fendorf, S., Planer-Friedrich, B., 2020. Arsenic Fate in Peat Controlled by the pH-Dependent Role of Reduced Sulfur. Environ. Sci. Technol. 54, 6682–6692. https://doi.org/10.1021/acs.est.0c00457

EC, 2015. European Commission Directive 2015/1787 of 6 October 2015 amending Annexes II and III to Council Directive 98/83/EC on the quality of water intended for human consumption.

Erickson, M.L., Barnes, R.J., 2005. Well characteristics influencing arsenic concentrations in ground water. Water Res. 39, 4029–4039. https://doi.org/10.1016/j.watres.2005.07.026

Ersbøll, A.K., Monrad, M., Sørensen, M., Baastrup, R., Hansen, B., Bach, F.W., Tjønneland, A., Overvad, K., Raaschou-Nielsen, O., 2018. Low-level exposure to arsenic in drinking water and incidence rate of stroke: A cohort study in Denmark. Environ. Int. 120, 72–80. https://doi.org/10.1016/j.envint.2018.07.040

Fendorf, S., Michael, H.A., van Geen, A., 2010. Spatial and Temporal Variations of Groundwater Arsenic in South and Southeast Asia. Science 328, 1123–1127. https://doi.org/10.1126/science.1172974

Fritz, S.J., 1994. A Survey of Charge-Balance Errors on Published Analyses of Potable Ground and Surface Waters. Groundwater 32, 539–546. https://doi.org/10.1111/j.1745-6584.1994.tb00888.x

Gerritse, R.G., George, R.J., 1988. The role of soil organic matter in the geochemical cycling of chloride and bromide. J. Hydrol. 101, 83–95. https://doi.org/10.1016/0022-1694(88)90029-7

Giuliano, G., 1995. Ground water in the Po basin: some problems relating to its use and protection. Sci. Total Environ. 171, 17–27. https://doi.org/10.1016/0048-9697(95)04682-1

Gyuró, É.K., 2007. The Pannonian Great Plain a flourishing garden?: Water as a key to the history and future of the central lowlands in the Carpathian basin. In: Pedroli, B., van Doorn, A., de Blust, G., (Eds.), Europe's Living Landscapes. KNNV Publishing, Leiden, pp. 294–309. https://doi.org/10.1163/9789004278073_019

Hansen, L.K., Jakobsen, R., Postma, D., 2001. Methanogenesis in a shallow sandy aquifer, Rømø, Denmark. Geochim. Cosmochim. Acta 65, 2925–2935. https://doi.org/10.1016/S0016-7037(01)00653-6

Hoehler, T.M., 2004. Biological energy requirements as quantitative boundary conditions for life in the subsurface.

Geobiology 2, 205–215. https://doi.org/10.1111/j.1472-4677.2004.00033.x

Hoehler, T.M., Alperin, M.J., Albert, D.B., Martens, C.S., 2001. Apparent minimum free energy requirements for methanogenic Archaea and sulfate-reducing bacteria in an anoxic marine sediment. FEMS Microbiol. Ecol. 38, 33–41. https://doi.org/10.1111/j.1574-6941.2001.tb00879.x

Hoehler, T.M., Alperin, M.J., Albert, D.B., Martens, C.S., 1994. Field and Laboratory Studies of Methane Oxidation in an Anoxic Marine Sediment: Evidence for a Methanogen-Sulfate Reducer Consortium. Global Biogeochem. Cy. 8, 451–463. https://doi.org/10.1029/94GB01800

Jakobsen, R., 2007. Redox microniches in groundwater: A model study on the geometric and kinetic conditions required for concomitant Fe oxide reduction, sulfate reduction, and methanogenesis. Water Resour. Res. 43, W12S12. https://doi.org/10.1029/2006WR005663

Jakobsen, R., Cold, L., 2007. Geochemistry at the sulfate reduction–methanogenesis transition zone in an anoxic aquifer—A partial equilibrium interpretation using 2D reactive transport modeling. Geochim. Cosmochim. Acta 71, 1949–1966. https://doi.org/10.1016/J.GCA.2007.01.013

Jin, Q., Bethke, C.M., 2009. Cellular energy conservation and the rate of microbial sulfate reduction. Geology 37, 1027–1030. https://doi.org/10.1130/G30185A.1

Jin, Q., Bethke, C.M., 2003. A New Rate Law Describing Microbial Respiration. Appl. Environ. Microbiol. 69, 2340–2348. https://doi.org/10.1128/AEM.69.4.2340-2348.2003

Kelly, W.R., Holm, T.R., Wilson, S.D., Roadcap, G.S., 2005. Arsenic in Glacial Aquifers: Sources and Geochemical Controls. Groundwater 43, 500–510. https://doi.org/10.1111/j.1745-6584.2005.0058.x

Kirk, M.F., Holm, T.R., Park, J., Jin, Q., Sanford, R.A., Fouke, B.W., Bethke, C.M., 2004. Bacterial sulfate reduction limits natural arsenic contamination in groundwater. Geology 32, 953–956. https://doi.org/10.1130/G20842.1

Kocar, B.D., Benner, S.G., Fendorf, S., 2014. Deciphering and predicting spatial and temporal concentrations of arsenic within the Mekong Delta aquifer. Environ. Chem. 11, 579–594. https://doi.org/10.1071/EN13244

Langner, P., Mikutta, C., Kretzschmar, R., 2012. Arsenic sequestration by organic sulphur in peat. Nat. Geosci. 5, 66–73. https://doi.org/10.1038/ngeo1329

Lindquist, S.J., 1999. Petroleum systems of the Po Basin Province of northern Italy and the northern Adriatic Sea; Porto Garibaldi (biogenic), Meride/Riva di Solto (thermal), and Marnoso Arenacea (thermal). U.S. Geological Survey Open-File Report 99-50-M. https://doi.org/10.3133/ofr9950M

Lovley, D.R., 1987. Organic matter mineralization with the reduction of ferric iron: A review. Geomicrobiol. J. 5, 375–399. https://doi.org/10.1080/01490458709385975

Lovley, D.R., Goodwin, S., 1988. Hydrogen concentrations as an indicator of the predominant terminal electron-accepting reactions in aquatic sediments. Geochim. Cosmochim. Acta 52, 2993–3003. https://doi.org/10.1016/0016-7037(88)90163-9

Maesano, F.E., D'Ambrogi, C., 2016. Coupling sedimentation and tectonic control: Pleistocene evolution of the central Po Basin. Ital. J. Geosci. 135, 394–407. https://doi.org/10.3301/IJG.2015.17

Marchetti, M., 2002. Environmental changes in the central Po Plain (northern Italy) due to fluvial modifications and anthropogenic activities. Geomorphology 44, 361–373. https://doi.org/10.1016/S0169-555X(01)00183-0

Martinelli, G., Chahoud, A., Dadomo, A., Fava, A., 2014. Isotopic features of Emilia-Romagna region (North Italy) groundwaters: Environmental and climatological implications. J. Hydrol. 519, 1928–1938. https://doi.org/10.1016/J.JHYDROL.2014.09.077

Mattavelli, L., Novelli, L., 1988. Geochemistry and habitat of natural gases in Italy. Org. Geochem. 13, 1–13. https://doi.org/10.1016/0146-6380(88)90021-6

Mattavelli, L., Ricchiuto, T., Grignani, D., Schoell, M., 1983. Geochemistry and Habitat of Natural Gases in Po Basin, Northern Italy. Am. Assoc. Pet. Geol. Bull. 67, 2239–2254.

McArthur, J.M., 2019. Arsenic in Groundwater, in: Sikdar, P.K. (Ed.), Groundwater Development and Management: Issues and Challenges in South Asia. Springer International Publishing, Cham, pp. 279–308. https://doi.org/10.1007/978-3-319-75115-3_12

McArthur, J.., Banerjee, D.., Hudson-Edwards, K.., Mishra, R., Purohit, R., Ravenscroft, P., Cronin, A., Howarth, R.., Chatterjee, A., Talukder, T., Lowry, D., Houghton, S., Chadha, D.., 2004. Natural organic matter in sedimentary basins and its relation to arsenic in anoxic ground water: the example of West Bengal and its worldwide implications. Appl. Geochem. 19, 1255–1293. https://doi.org/10.1016/J.APGEOCHEM.2004.02.001

McArthur, J.M., Ravenscroft, P., Banerjee, D.M., Milsom, J., Hudson-Edwards, K.A., Sengupta, S., Bristow, C., Sarkar, A., Tonkin, S., Purohit, R., 2008. How paleosols influence groundwater flow and arsenic pollution: A model from the Bengal Basin and its worldwide implication. Water Resour. Res. 44, W11411. https://doi.org/10.1029/2007WR006552

McArthur, J.M., Ghosal, U., Sikdar, P.K., Ball, J.D., 2016. Arsenic in Groundwater: The Deep Late Pleistocene Aquifers of the Western Bengal Basin. Environ. Sci. Technol. 50, 3469–3476. https://doi.org/10.1021/acs.est.5b02477

McMahon, P.B., Chapelle, F.H., 1991. Microbial production of organic acids in aquitard sediments and its role in aquifer geochemistry. Nature 349, 233–235. https://doi.org/10.1038/349233a0

McMahon, P.B., Chapelle, F.H., 2008. Redox Processes and Water Quality of Selected Principal Aquifer Systems.

Groundwater 46, 259–271. https://doi.org/10.1111/j.1745-6584.2007.00385.x

Meliker, J.R., Slotnick, M.J., Avruskin, G.A., Haack, S.K., Nriagu, J.O., 2008. Influence of groundwater recharge and well characteristics on dissolved arsenic concentrations in southeastern Michigan groundwater. Environ. Geochem. Health 31, 147. https://doi.org/10.1007/s10653-008-9173-x

Mihajlov, I., Mozumder, M.R.H., Bostick, B.C., Stute, M., Mailloux, B.J., Knappett, P.S.K., Choudhury, I., Ahmed, K.M., Schlosser, P., van Geen, A., 2020. Arsenic contamination of Bangladesh aquifers exacerbated by clay layers. Nat. Commun. 11, 2244. https://doi.org/10.1038/s41467-020-16104-z

Milkov, A. V, Etiope, G., 2018. Revised genetic diagrams for natural gases based on a global dataset of >20,000 samples. Org. Geochem. 125, 109–120. https://doi.org/10.1016/j.orggeochem.2018.09.002

Miola, A., Bondesan, A., Corain, L., Favaretto, S., Mozzi, P., Piovan, S., Sostizzo, I., 2006. Wetlands in the Venetian Po Plain (northeastern Italy) during the Last Glacial Maximum: Interplay between vegetation, hydrology and sedimentary environment. Rev. Palaeobot. Palynol. 141, 53–81. https://doi.org/10.1016/J.REVPALBO.2006.03.016

Molinari, A., Ayora, C., Marcaccio, M., Guadagnini, L., Sanchez-Vila, X., Guadagnini, A., 2014. Geochemical modeling of arsenic release from a deep natural solid matrix under alternated redox conditions. Environ. Sci. Pollut. Res. 21, 1628–1637. https://doi.org/10.1007/s11356-013-2054-6

Molinari, A., Guadagnini, L., Marcaccio, M., Guadagnini, A., 2015. Arsenic fractioning in natural solid matrices sampled in a deep groundwater body. Geoderma 247–248, 88–96. https://doi.org/10.1016/j.geoderma.2015.02.011

Molinari, A., Guadagnini, L., Marcaccio, M., Straface, S., Sanchez-Vila, X., Guadagnini, A., 2013. Arsenic release from deep natural solid matrices under experimentally controlled redox conditions. Sci. Total Environ. 444, 231–240. https://doi.org/10.1016/J.SCITOTENV.2012.11.093

Murphy, E.M., Schramke, J.A., Fredrickson, J.K., Bledsoe, H.W., Francis, A.J., Sklarew, D.S., Linehan, J.C., 1992. The influence of microbial activity and sedimentary organic carbon on the isotope geochemistry of the Middendorf Aquifer. Water Resour. Res. 28, 723–740. https://doi.org/10.1029/91WR02678

Nickson, R., McArthur, J., Burgess, W., Ahmed, K.M., Ravenscroft, P., Rahmanñ, M., 1998. Arsenic poisoning of Bangladesh groundwater. Nature 395, 338. https://doi.org/10.1038/26387

O'Day, P.A., Vlassopoulos, D., Root, R., Rivera, N., 2004. The influence of sulfur and iron on dissolved arsenic concentrations in the shallow subsurface under changing redox conditions. Proc. Natl. Acad. Sci. U. S. A. 101, 13703–13708. https://doi.org/10.1073/pnas.0402775101

Ori, G.G., 1993. Continental depositional systems of the Quaternary of the Po Plain (northern Italy). Sediment. Geol. 83,

1–14. https://doi.org/10.1016/S0037-0738(10)80001-6

Parkhurst, D.L., Appelo, C.A.J., 2013. Description of input and examples for PHREEQC version 3: A computer program for speciation, batch-reaction, one-dimensional transport, and inverse geochemical calculations. U. S. Geological Survey Techniques and Methods 6-A4, Book 6, Chapter 43.

Perego, R., Bonomi, T., Fumagalli, M.L., Benastini, V., Aghib, F., Rotiroti, M., Cavallin, A., 2014. 3D reconstruction of the multi-layer aquifer in a Po Plain area. Rend. Online Soc. Geol. Ital. 30, 41–44. https://doi.org/10.3301/ROL.2014.09

Planer-Friedrich, B., Härtig, C., Lissner, H., Steinborn, J., Süß, E., Qumrul Hassan, M., Zahid, A., Alam, M., Merkel, B., 2012. Organic carbon mobilization in a Bangladesh aquifer explained by seasonal monsoon-driven storativity changes. Appl. Geochem. 27, 2324–2334. https://doi.org/10.1016/j.apgeochem.2012.08.005

Postma, D., 1982. Pyrite and siderite formation in brackish and freshwater swamp sediments. Am. J. Sci. 282, 1151–1183. https://doi.org/10.2475/ajs.282.8.1151

Postma, D., Jakobsen, R., 1996. Redox zonation: Equilibrium constraints on the Fe(III)/SO4-reduction interface. Geochim. Cosmochim. Acta 60, 3169–3175. https://doi.org/10.1016/0016-7037(96)00156-1

Postma, D., Larsen, F., Minh Hue, N.T., Duc, M.T., Viet, P.H., Nhan, P.Q., Jessen, S., 2007. Arsenic in groundwater of the Red River floodplain, Vietnam: Controlling geochemical processes and reactive transport modeling. Geochim. Cosmochim. Acta 71, 5054–5071. https://doi.org/10.1016/J.GCA.2007.08.020

Postma, D., Larsen, F., Thai, N.T., Trang, P.T.K., Jakobsen, R., Nhan, P.Q., Long, T.V., Viet, P.H., Murray, A.S., 2012. Groundwater arsenic concentrations in Vietnam controlled by sediment age. Nat. Geosci. 5, 656–661. https://doi.org/10.1038/ngeo1540

Radloff, K.A., Zheng, Y., Stute, M., Weinman, B., Bostick, B., Mihajlov, I., Bounds, M., Rahman, M.M., Huq, M.R., Ahmed, K.M., Schlosser, P., van Geen, A., 2017. Reversible adsorption and flushing of arsenic in a shallow, Holocene aquifer of Bangladesh. Appl. Geochem. 77, 142–157. https://doi.org/10.1016/j.apgeochem.2015.11.003

Ravenscroft, P., Brammer, H., Richards, K., 2009. Arsenic Pollution: A Global Synthesis. Wiley-Blackwell, Chichester. https://doi.org/10.1002/9781444308785

Ravenscroft, P., McArthur, J.M., Hoque, B.A., 2001. Geochemical and Palaeohydrological Controls on Pollution of Groundwater by Arsenic., in: Chappell, W.R., Abernathy, C.O., Calderon, R.L. (Eds.), Arsenic Exposure and Health Effects IV. Elsevier Science Ltd, Oxford, pp. 53–78.

Richards, L.A., Magnone, D., Sültenfuß, J., Chambers, L., Bryant, C., Boyce, A.J., van Dongen, B.E., Ballentine, C.J., Sovann, C., Uhlemann, S., Kuras, O., Gooddy, D.C., Polya, D.A., 2019. Dual in-aquifer and near surface processes

drive arsenic mobilization in Cambodian groundwaters. Sci. Total Environ. 659, 699–714. https://doi.org/10.1016/j.scitotenv.2018.12.437

Rossi, M., Minervini, M., Ghielmi, M., Rogledi, S., 2015. Messinian and Pliocene erosional surfaces in the Po Plain-Adriatic Basin: Insights from allostratigraphy and sequence stratigraphy in assessing play concepts related to accommodation and gateway turnarounds in tectonically active margins. Mar. Pet. Geol. 66, 192–216. https://doi.org/10.1016/j.marpetgeo.2014.12.012

Rotiroti, M., Bonomi, T., Sacchi, E., McArthur, J.M., Stefania, G.A., Zanotti, C., Taviani, S., Patelli, M., Nava, V., Soler, V., Fumagalli, L., Leoni, B., 2019a. The effects of irrigation on groundwater quality and quantity in a human-modified hydro-system: The Oglio River basin, Po Plain, northern Italy. Sci. Total Environ. 672, 342–356. https://doi.org/10.1016/J.SCITOTENV.2019.03.427

Rotiroti, M., Jakobsen, R., Fumagalli, L., Bonomi, T., 2018. Considering a threshold energy in reactive transport modeling of microbially mediated redox reactions in an arsenic-affected aquifer. Water 10, 90. https://doi.org/10.3390/w10010090

Rotiroti, M., Jakobsen, R., Fumagalli, L., Bonomi, T., 2015. Arsenic release and attenuation in a multilayer aquifer in the Po Plain (northern Italy): Reactive transport modeling. Appl. Geochem. 63, 599–609. https://doi.org/10.1016/j.apgeochem.2015.07.001

Rotiroti, M., McArthur, J., Fumagalli, L., Stefania, G.A., Sacchi, E., Bonomi, T., 2017. Pollutant sources in an arsenic-affected multilayer aquifer in the Po Plain of Italy: Implications for drinking-water supply. Sci. Total Environ. 578, 502–512. https://doi.org/10.1016/j.scitotenv.2016.10.215

Rotiroti, M., Sacchi, E., Fumagalli, L., Bonomi, T., 2014. Origin of arsenic in groundwater from the multilayer aquifer in cremona (Northern Italy). Environ. Sci. Technol. 48, 5395–5403. https://doi.org/10.1021/es405805v

Rotiroti, M., Zanotti, C., Fumagalli, L., Taviani, S., Stefania, G.A., Patelli, M., Nava, V., Soler, V., Sacchi, E., Leoni, B., 2019b. Multivariate statistical analysis supporting the hydrochemical characterization of groundwater and surface water: A case study in northern Italy. Rend. Online Soc. Geol. Ital. 47, 90–96. https://doi.org/10.3301/ROL.2019.17

Rowland, H.A.L., Omoregie, E.O., Millot, R., Jimenez, C., Mertens, J., Baciu, C., Hug, S.J., Berg, M., 2011. Geochemistry and arsenic behaviour in groundwater resources of the Pannonian Basin (Hungary and Romania). Appl. Geochem. 26, 1–17. https://doi.org/10.1016/J.APGEOCHEM.2010.10.006

Sciarra, A., Cinti, D., Pizzino, L., Procesi, M., Voltattorni, N., Mecozzi, S., Quattrocchi, F., 2013. Geochemistry of shallow aquifers and soil gas surveys in a feasibility study at the Rivara natural gas storage site (Po Plain, Northern Italy). Appl. Geochem. 34, 3–22. https://doi.org/10.1016/J.APGEOCHEM.2012.11.008

Sø, H.U., Postma, D., Vi, M.L., Pham, T.K.T., Kazmierczak, J., Dao, V.N., Pi, K., Koch, C.B., Pham, H.V., Jakobsen, R., 2018. Arsenic in Holocene aquifers of the Red River floodplain, Vietnam: Effects of sediment-water interactions, sediment burial age and groundwater residence time. Geochim. Cosmochim. Acta 225, 192–209. https://doi.org/10.1016/J.GCA.2018.01.010

Sracek, O., Berg, M., Müller, B., 2018. Redox buffering and de-coupling of arsenic and iron in reducing aquifers across the Red River Delta, Vietnam, and conceptual model of de-coupling processes. Environ. Sci. Pollut. Res. 25, 15954–15961. https://doi.org/10.1007/s11356-018-1801-0

Stuckey, J.W., Schaefer, M.V., Kocar, B.D., Benner, S.G., Fendorf, S., 2016. Arsenic release metabolically limited to permanently water-saturated soil in Mekong Delta. Nat. Geosci. 9, 70–76. https://doi.org/10.1038/ngeo2589

Sutton, N.B., van der Kraan, G.M., van Loosdrecht, M.C.M., Muyzer, G., Bruining, J., Schotting, R.J., 2009. Characterization of geochemical constituents and bacterial populations associated with As mobilization in deep and shallow tube wells in Bangladesh. Water Res. 43, 1720–1730. https://doi.org/10.1016/J.WATRES.2009.01.006

Wang, Y.H., Li, P., Dai, X.Y., Zhang, R., Jiang, Z., Jiang, D.W., Wang, Y.X., 2015. Abundance and diversity of methanogens: Potential role in high arsenic groundwater in Hetao Plain of Inner Mongolia, China. Sci. Total Environ. 515–516, 153–161. https://doi.org/10.1016/J.SCITOTENV.2015.01.031

Welch, A.H., Westjohn, D.B., Helsel, D.R., Wanty, R.B., 2000. Arsenic in Ground Water of the United States: Occurrence and Geochemistry. Groundwater 38, 589–604. https://doi.org/10.1111/j.1745-6584.2000.tb00251.x

Whiticar, M.J., 1999. Carbon and hydrogen isotope systematics of bacterial formation and oxidation of methane. Chem. Geol. 161, 291–314. https://doi.org/10.1016/S0009-2541(99)00092-3

WHO, 2011. Guidelines for drinking-water quality, 4th edition. World Health Organization, Geneva.

Winkel, L.H.E., Trang, P.T.K., Lan, V.M., Stengel, C., Amini, M., Ha, N.T., Viet, P.H., Berg, M., 2011. Arsenic pollution of groundwater in Vietnam exacerbated by deep aquifer exploitation for more than a century. Proc. Natl. Acad. Sci. U. S. A. 108, 1246–1251. https://doi.org/10.1073/pnas.1011915108

Yao, H., Conrad, R., 1999. Thermodynamics of Methane Production in Different Rice Paddy Soils from China, the Philippines and Italy. Soil Biol. Biochem. 31, 463–473; https://doi.org/10.1016/S0038-0717(98)00152-7

Zanotti, C., Rotiroti, M., Fumagalli, L., Stefania, G.A., Canonaco, F., Stefenelli, G., Prévôt, A.S.H., Leoni, B., Bonomi, T., 2019. Groundwater and surface water quality characterization through positive matrix factorization combined with GIS approach. Water Res. 159, 122–134. https://doi.org/10.1016/j.watres.2019.04.058

Zhou, S., Xu, J., Yang, G., Zhuang, L., 2014. Methanogenesis affected by the co-occurrence of iron(III) oxides and humic substances. FEMS Microbiol. Ecol. 88, 107–120. https://doi.org/10.1111/1574-6941.12274

Zuppi, G.M., Sacchi, E., 2004. Hydrogeology as a climate recorder: Sahara–Sahel (North Africa) and the Po Plain (Northern Italy). Glob. Planet. Change 40, 79–91. https://doi.org/10.1016/S0921-8181(03)00099-7

Zuzolo, D., Cicchella, D., Demetriades, A., Birke, M., Albanese, S., Dinelli, E., Lima, A., Valera, P., De Vivo, B., 2020. Arsenic: Geochemical distribution and age-related health risk in Italy. Environ. Res. 182, 109076. https://doi.org/10.1016/J.ENVRES.2019.109076

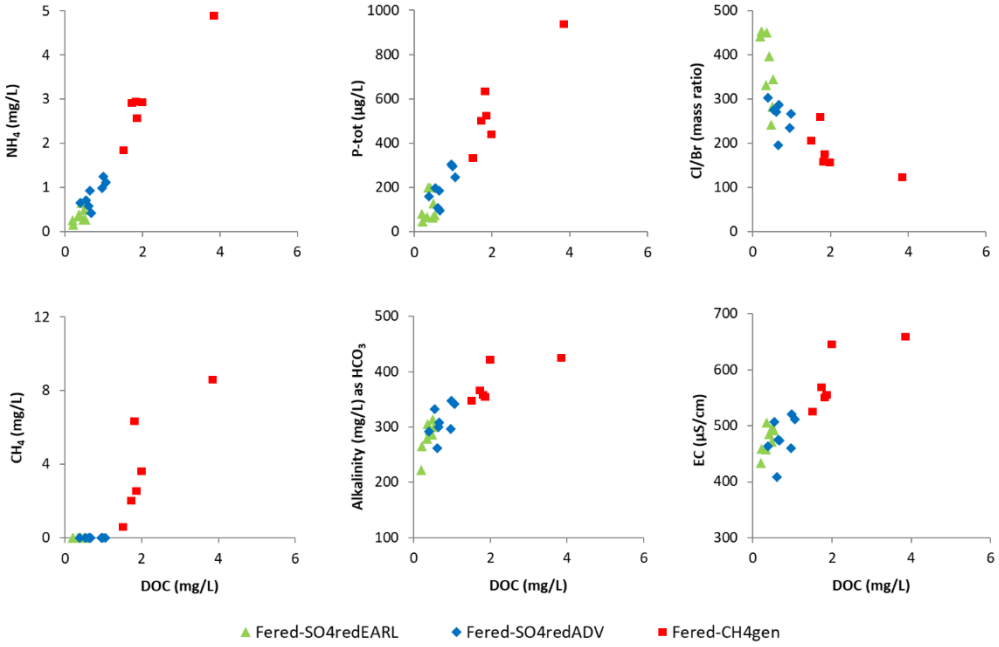

Fig. 1. Scatter plots of DOC vs NH_4, total phosphorus (P-tot), Cl/Br, CH_4, alkalinity, and EC. Fered-SO4redEARL: groundwaters under Fe-oxide reduction and early-stage sulfate reduction; Fered-SO4redADV: groundwaters under Fe-oxide reduction and advanced-stage sulfate reduction; Fered-CH4gen: groundwaters under Fe-oxide reduction and methanogenesis.

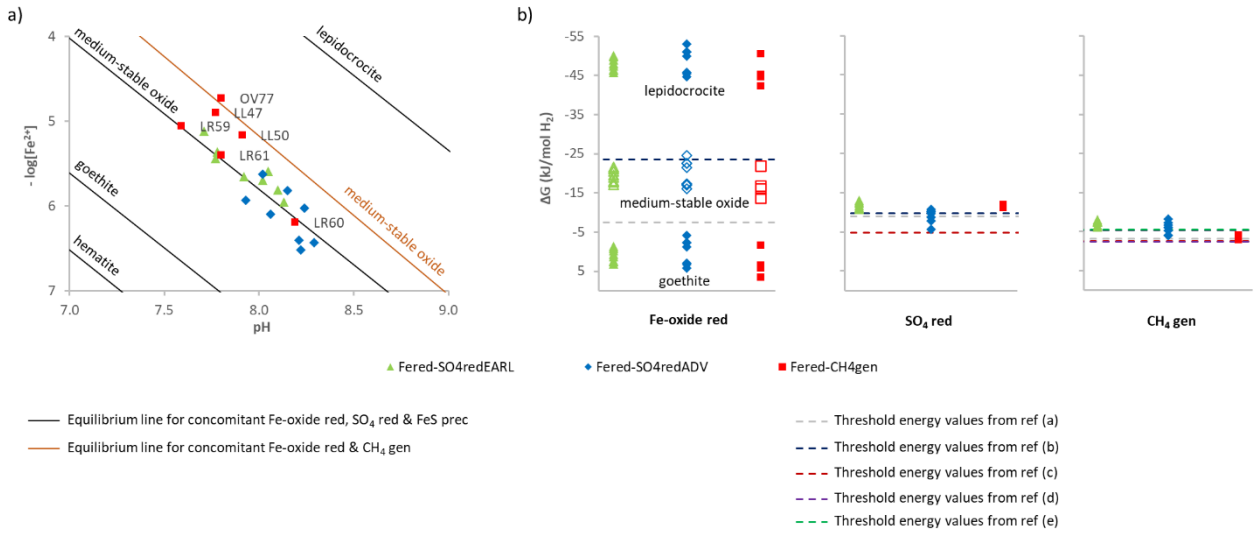

Fig. 2. Testing the "partial" equilibrium state in the studied system. a) Equilibrium diagram of the simultaneous equilibrium of Fe-oxide reduction, sulfate reduction and FeS precipitation (black lines), and Fe-oxide reduction and methanogenesis (orange line) for different Fe-oxides; see Table S4 for reactions and equilibrium line equations. The equilibrium lines are plotted considering a value of −3 for $\log[SO_4^{2-}]$, according to Postma and Jakobsen (1996), and average measured values of −2.35 for $\log[HCO_3^-]$ and −6.21 for $\log[CH_4]$. b) Computed available energy at system conditions (symbols) over threshold energy (dotted lines) for Fe-oxide reduction, sulfate reduction and methanogenesis; threshold energy values are from (a) Rotiroti et al., 2018 (b) Jakobsen and Cold, 2007 (c) Hoehler et al., 2001 (d) Hoehler et al., 1994 (e) Yao and Conrad, 1999. Fered-SO4redEARL: groundwaters under Fe-oxide reduction and early-stage sulfate reduction; Fered-SO4redADV: groundwaters under Fe-oxide reduction and advanced-stage sulfate reduction; Fered-CH4gen: groundwaters under Fe-oxide reduction and methanogenesis.

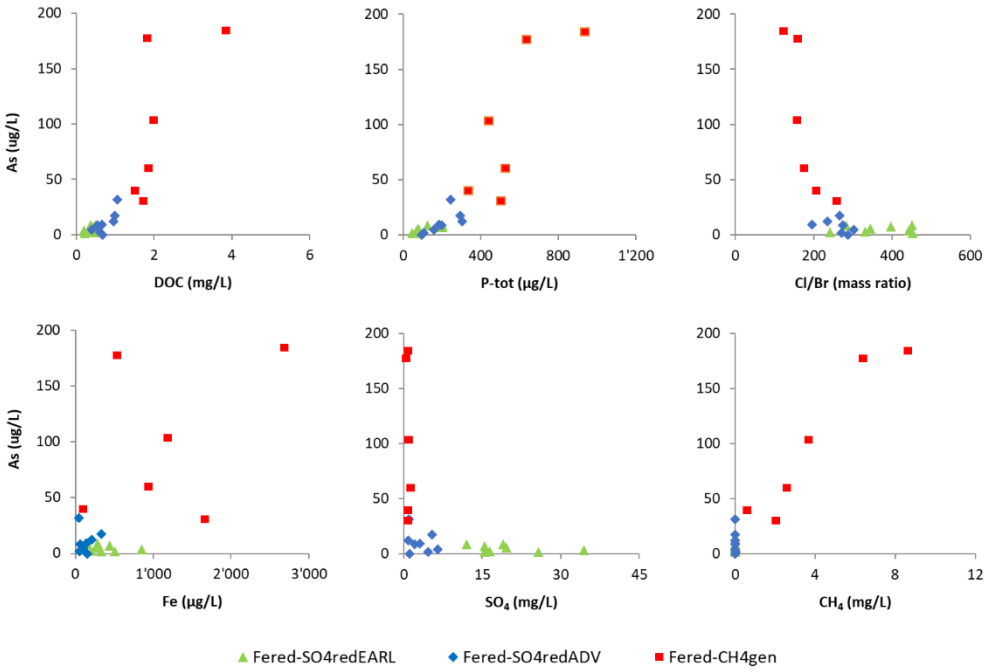

Fig. 3. Scatter plots of As vs DOC, total phosphorus (P-tot), Cl/Br, Fe, SO_4 and CH_4. Fered-SO4redEARL: groundwaters under Fe-oxide reduction and early-stage sulfate reduction; Fered-SO4redADV: groundwaters under Fe-oxide reduction and advanced-stage sulfate reduction; Fered-CH4gen: groundwaters under Fe-oxide reduction and methanogenesis.

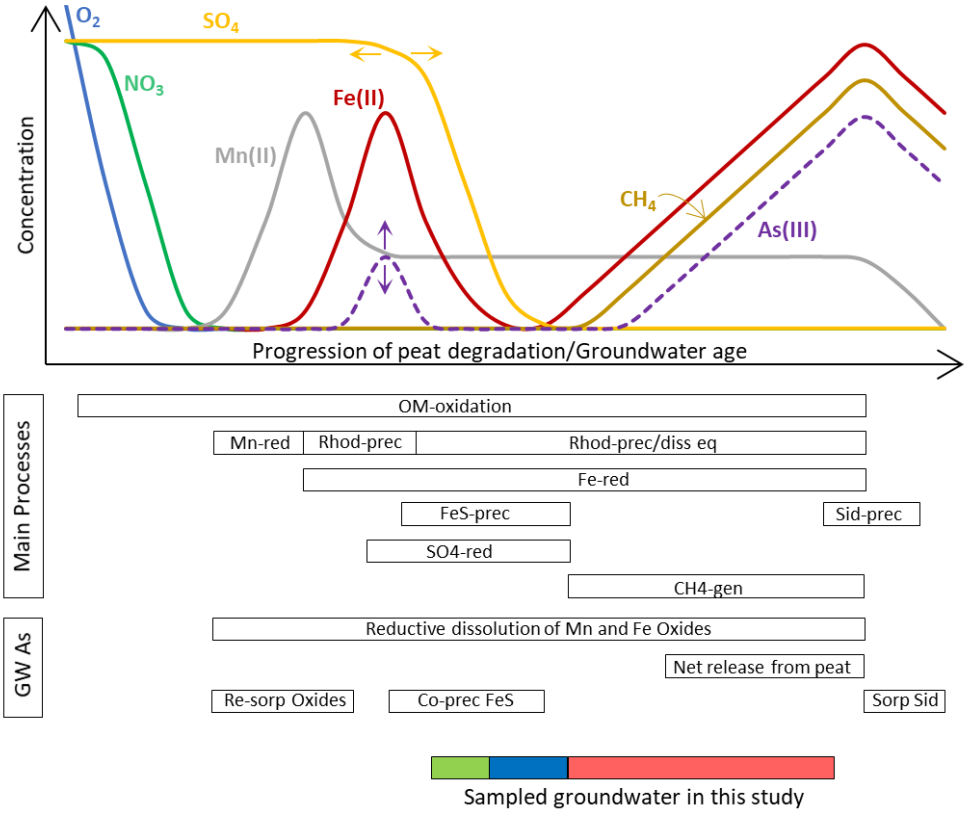

Fig. 4. Schematization of the evolution of the concentration of As and the main redox-sensitive species, together with related main processes, with the progression of peat degradation; see the text for a detailed explanation. For the bar "Sampled groundwater in this study", the green part refers to samples classified under Fe-oxide reduction and early-stage sulfate reduction, the blue refers to Fe-oxide reduction and advanced-stage sulfate reduction, and the red to Fe-oxide reduction and methanogenesis.

Overlapping redox zones control arsenic pollution in Pleistocene multi-layer aquifers, the Po Plain (Italy)

Supporting Information

Marco Rotiroti[1], Tullia Bonomi[1], Elisa Sacchi[2], John M. McArthur[3], Rasmus Jakobsen[4], Alessandra Sciarra[5], Giuseppe Etiope[6], Chiara Zanotti[1], Veronica Nava[1], Letizia Fumagalli[1] and Barbara Leoni[1]*

[1]*Department of Earth and Environmental Sciences, University of Milano-Bicocca, Milan, Italy.*
[2]*Department of Earth and Environmental Sciences, University of Pavia, Pavia, Italy.*
[3]*Department of Earth Sciences, University College London, London, United Kingdom.*
[4]*Geological Survey of Denmark and Greenland, Copenhagen, Denmark.*
[5]*Istituto Nazionale di Geofisica e Vulcanologia, Sezione Roma 1, Rome, Italy.*
[6]*Istituto Nazionale di Geofisica e Vulcanologia, Sezione Roma 2, Rome, Italy.*
**corresponding author, email: marco.rotiroti@unimib.it, tel: +39 0264482882.*

Content:

Number of pages: 15
Number of sections: 6
Number of figures: 10
Number of tables: 4
Number of references: 18

Section S1. Additional figures

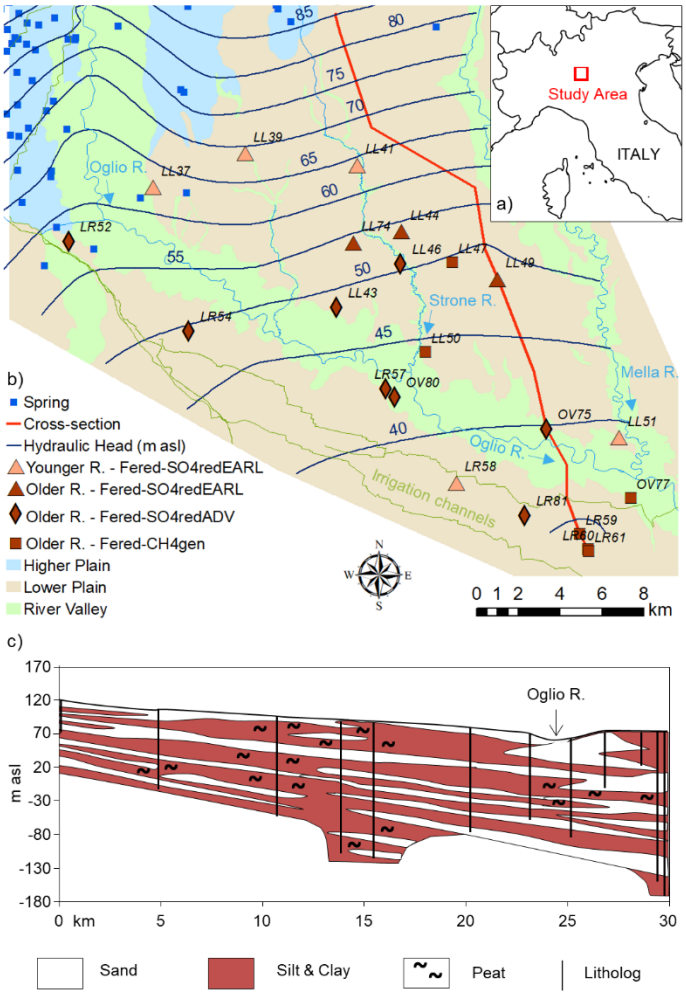

Fig. S1. a) Location of the study area. b) Location of sampling points classified on type of recharge and redox state (see the text for details) with surface water bodies, potentiometric map for deeper (>40 m bgs) aquifers (Rotiroti et al., 2019), geomorphological units (Regione Lombardia, 2019) and location of the cross-section. c) Lithological cross-section, modified from Rotiroti et al. (2019).

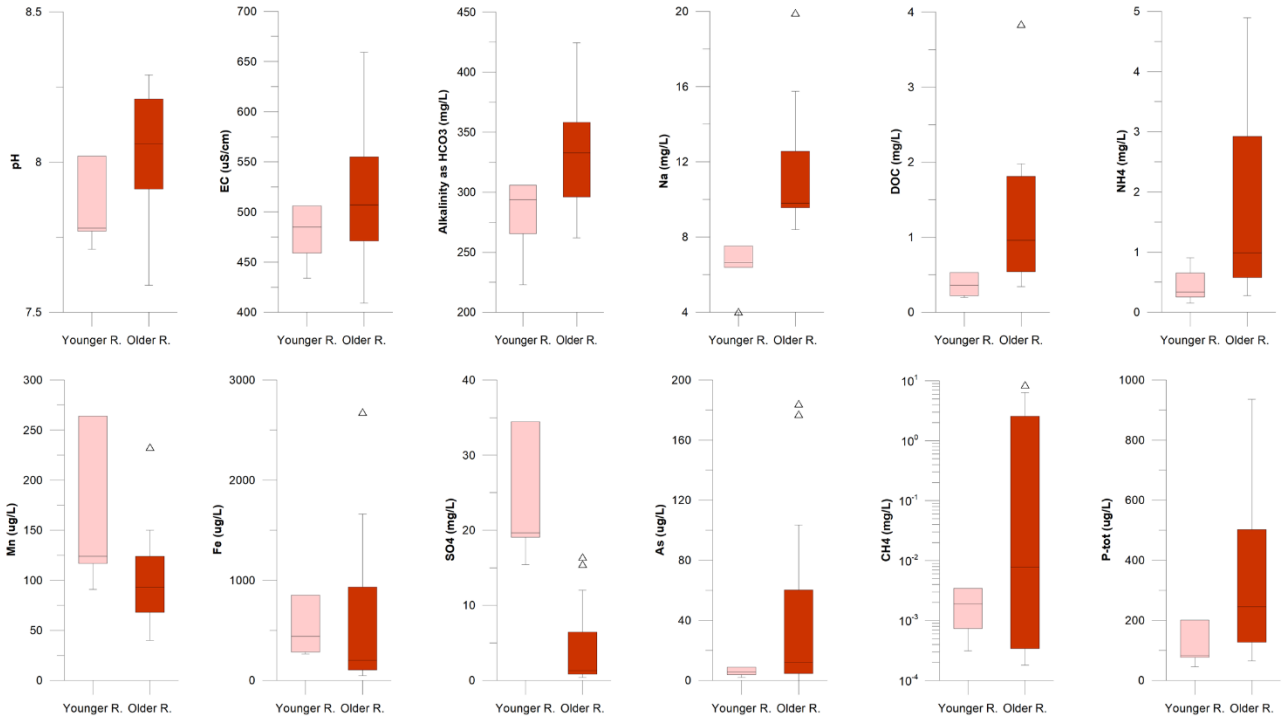

Fig. S2. Box-plot graphs of measured values for selected parameters with samples classified in groundwaters having a component of younger recharge (Younger R.; with Cl/Br >340 and δ^2H <−60‰) and groundwaters with older recharge (Older R.; with Cl/Br <340 and δ^2H >−60‰).

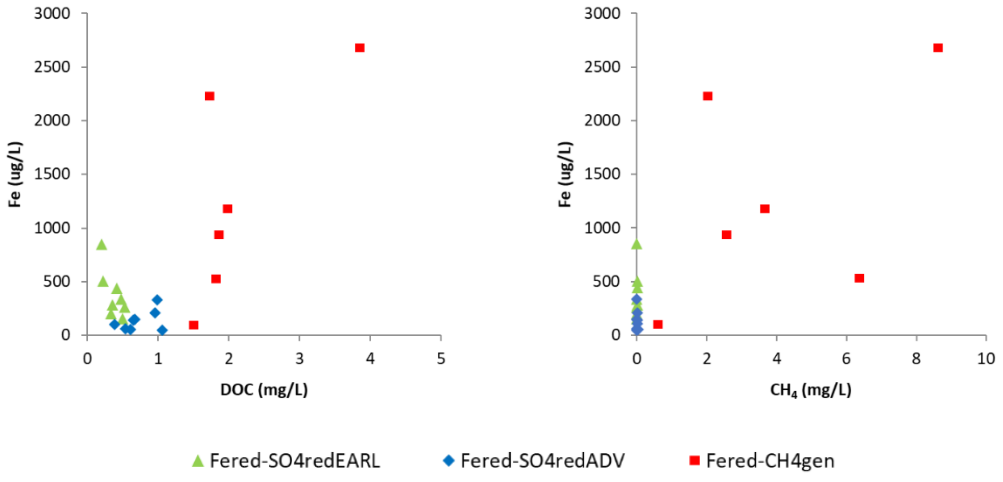

Fig. S3. Scatter plots of Fe vs DOC and CH_4. Fered-SO4redEARL: groundwaters under Fe-oxide reduction and early-stage sulfate reduction; Fered-SO4redADV: groundwaters under Fe-oxide reduction and advanced-stage sulfate reduction; Fered-CH4gen: groundwaters under Fe-oxide reduction and methanogenesis.

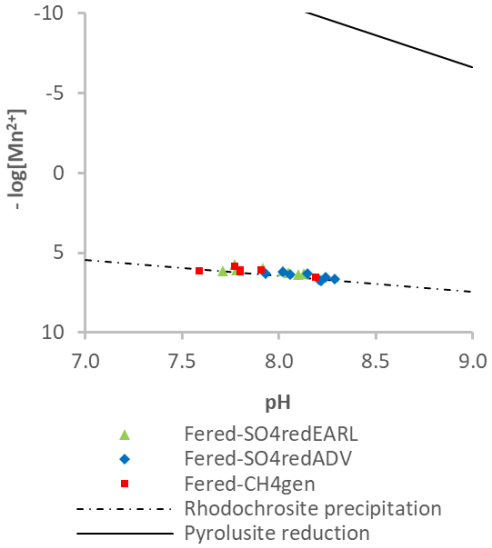

Fig. S4. Equilibrium diagram of Mn-oxide reduction and rhodochrosite precipitation. Equilibrium line equation is $-\log[Mn^{2+}] = 4pH + 2pe - logK$ for Mn-oxide reduction (logK is 41.38 for pyrolusite; Ball and Nordstrom, 1991) and $-\log[Mn^{2+}] = pH + \log[HCO_3^-] - logK$ for rhodochrosite precipitation (logK is −0.83; Ball and Nordstrom, 1991). The equilibrium lines are plotted considering a value of −0.67 for pe and −2.35 for $\log[HCO_3^-]$ (average measured values). Fered-SO4redADV: groundwaters under Fe-oxide reduction and advanced-stage sulfate reduction; Fered-CH4gen: groundwaters under Fe-oxide reduction and methanogenesis.

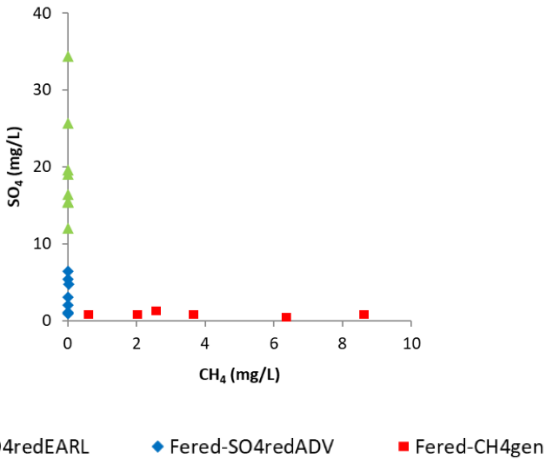

Fig. S5. Scatter plot of SO_4 vs CH_4. Fered-SO4redEARL: groundwaters under Fe-oxide reduction and early-stage sulfate reduction; Fered-SO4redADV: groundwaters under Fe-oxide reduction and advanced-stage sulfate reduction; Fered-CH4gen: groundwaters under Fe-oxide reduction and methanogenesis.

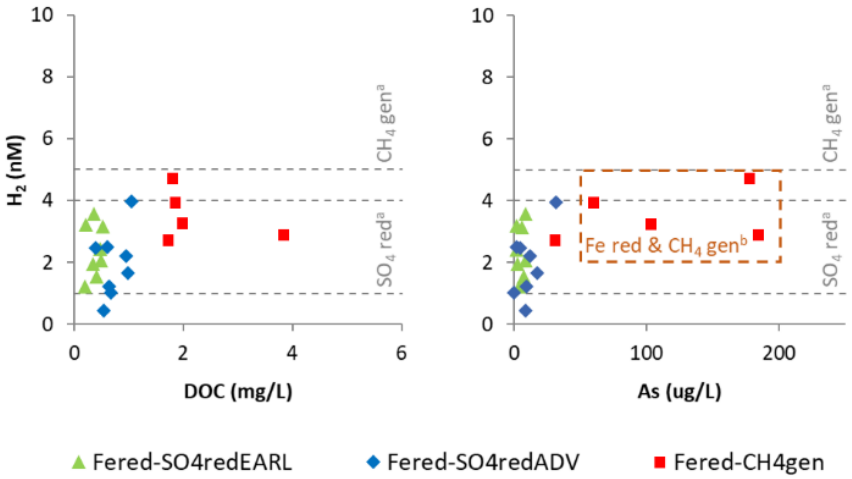

Fig. S6. Scatter plots of H_2 vs DOC and As. Dotted grey lines indicate H_2 ranges for sulfate reduction (1-4 nM) and methanogenesis (>5 nM) reported by [a]Chapelle et al. (1995); dotted orange box represents H_2/As ranges for samples of [b]Kirk et al. (2004) under concomitant Fe-Oxide reduction and methanogenesis. Fered-SO4redEARL: groundwaters under Fe-oxide reduction and early-stage sulfate reduction; Fered-SO4redADV: groundwaters under Fe-oxide reduction and advanced-stage sulfate reduction; Fered-CH4gen: groundwaters under Fe-oxide reduction and methanogenesis.

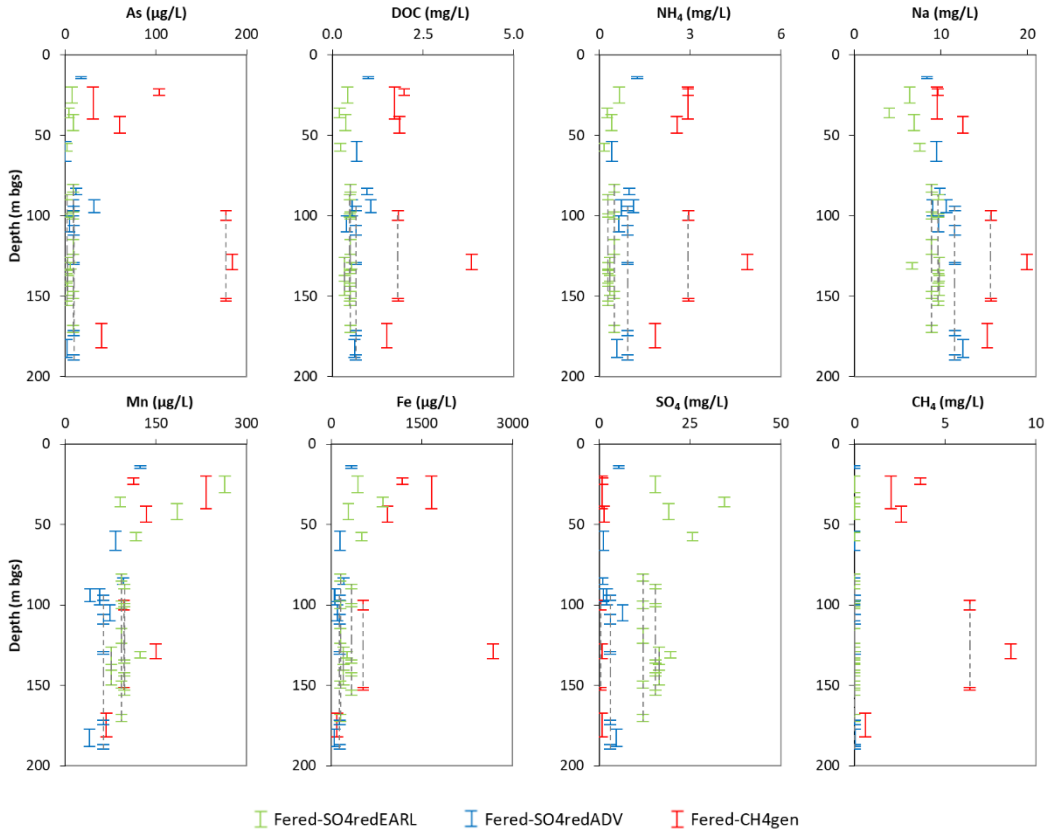

Fig. S7. Measured concentrations for selected parameters over depth. Length of symbols corresponds to length of well screen, dotted lines indicate multi-screen wells. Fered-SO4redEARL: groundwaters under Fe-oxide reduction and early-stage sulfate reduction; Fered-SO4redADV: groundwaters under Fe-oxide reduction and advanced-stage sulfate reduction; Fered-CH4gen: groundwaters under Fe-oxide reduction and methanogenesis.

Section S2. Additional tables

The following tables are reported in the attached file *Additional_Table.xls*

- Table S1. List of sampling points with measured parameters.

- Table S2. Stoichiometry of TEAP reactions (written as half reduction reaction) used for the calculation of Gibbs free energy of reaction; the electron donor is H_2, considered to come from the degradation of OM.

- Table S3. Pearson correlation coefficients matrix for all measured parameters.

- Table S4. Stoichiometry of TEAP reactions (written as half reduction reaction) and equilibrium line equations for concomitant equilibria considered in this study; the electron donor is e^-, considered to come from the oxidation of OM.

Section S3. Sampling operations, field measurements and laboratory analyses

Before sampling, wells were purged until water temperature, pH, EC, DO and ORP were constant. Samples were filtered in the field through 0.2 µm filters, those for trace elements (As, Fe and Mn), DOC and $\delta^{15}N$ in NH_4 analyses were acidified with nitric, phosphoric and hydrochloric acid, respectively. For CH_4 and H_2 analyses, unfiltered samples were collected in 200 mL serum bottles sealed with blue butyl rubber stoppers. The speciation of As (determination of As(III) and As(V)) was made for 14 samples by passing samples through As(V) retaining filter cartridges in the field (MetalSoft Centre®). Measurements of temperature, EC, pH, DO and ORP were made in the field using the WTW® Multi 3430 meter in a closed flow-cell. Alkalinity was analysed by sulfuric acid titration within 24 h of samples collection. Major ions were analysed by ion chromatography (Thermo Scientific® Dionex™ ICS-1100). Ammonium and total phosphorus were analysed by spectrophotometry (wavelengths at 690 and 882 nm, respectively; PerkinElmer® Lambda™ EZ 201) using the indophenol and molybdenum reactions, respectively. Iron and manganese were analysed by Inductively coupled plasma – optical emission spectroscopy (ICP-OES; PerkinElmer® Optima™ 7000 DV). Arsenic was analysed by graphite furnace atomic absorption spectrometry (GFAAS; PerkinElmer® AAnalyst™ 600). The DOC was analysed by high temperature catalytic combustion and infrared detection (Skalar® Formacs™ TOC/TN Analyzer). Dissolved gases (CH_4 and H_2) were extracted by using the methodology proposed by Capasso and Inguaggiato (1998) and analysed by gas chromatography (Varian® CP-4900 Micro-GC). Water isotopes ($\delta^{18}O$ & $\delta^{2}H$) and stable carbon isotope composition of methane ($\delta^{13}C$) were analysed by wavelength-scanned cavity ring-down spectroscopy (WS-CRDS; Picarro® L2120-I, water-, and Picarro® G2112-I, methane-, isotope analysers). Two methane standards of known stable C isotope composition (Isometric Instruments and Isotech calibrated atmospheric air), diluted to 2 and 1 ppmv, were used to trace the isotope measurements back to the Vienna Pee Dee Belemnite (VPDB) standard ($\delta^{13}C$, per mil, ‰). The $\delta^{15}N$ in ammonium was analysed by basification, steam distillation and sulfuric acid trapping as reported by Velinsky et al. (1989).

Section S4. Results and discussion of $\delta^{15}N_{NH4}$

Measured $\delta^{15}N$ values ranged from 11.3 to 16.0‰, except for well OV77 which had 1.3‰. These values are quite different from those reported by Rotiroti et al. (2017) in other areas of the Po Plain (Cremona, from 4.1 to 7.8‰) but are consistent with the range reported by Norrman et al. (2015) for deep reducing groundwaters in Vietnam (Nam Du, from 13 to 20‰). The value found for well OV77 is consistent with the values for buried peat reported by Norrman et al. (2015; 2-4‰) and Esmeijer-Liu et al. (2012; mean of −1.2‰ for pre-1950 peats).

Our values in most samples (i.e. between 11 and 16‰) are consistent with NH_4 originating from the mineralization of organic N contained in buried peat (which was reported to have $\delta^{15}N$ in the range 2-4‰; Norrman et al., 2015) that after dissociation to NH_3 and degassing, leads to an enrichment of the $\delta^{15}N$ values in the residual NH_4 (Norrman et al., 2015). The $\delta^{15}N_{NH4}$ value found in well OV77 (1.3‰), having the highest NH_4 concentration (4.89 mg/L), fits the range of parental organic N in peat and could be related to the fact that the screen of this well (9.5 m long, from 124 to 133.5 m bgs) intercepts a clay layer in the upper 2 m (from 124 to 126 m bgs). Groundwater closely interacting with clays (possibly peaty clays) could have higher NH_4 concentrations and a $\delta^{15}N$ in NH_4 that reflects the parental organic N in peat rather than being enriched by the dissociation/degassing processes. This is consistent with the $\delta^{15}N$ values for exchangeable NH_4 of the peat material that were reported by Norrman et al. (2015) to be 1-11‰. However, in aquifer systems with strong reducing groundwaters generated by the degradation of peat, the isotopic composition of NH_4 cannot be used alone to sustain its natural origin, since some anthropogenic sources of NH_4 have similar compositional range, i.e. animal manure is in the range 10-20‰ (Kendall, 1998; Kendall and Aravena, 2000; Nikolenko et al., 2018).

Section S5. Correlation of DOC with Na and Ca

An interesting side aspect is the positive correlation of Na and Ca, although weaker, with DOC (and thus with NH_4 and P-tot), that is shown in Fig. S8. This could be related to groundwater residence times: as the accumulated degradation of OM increases over time, leading to higher DOC and NH_4, also effects of water-rock (clay) interactions accumulate over time, possibly leading to higher Na and Ca. The increase of Ca could be due to Ca-feldspars and/or other Ca-bearing silicates, rather than calcite, slowly dissolving over time. The increase of Na, in pristine groundwater hosted by aquifer systems containing clay layers and with no saline or brackish water intrusion, can also be considered as the product of silicate mineral dissolution (Appelo and Postma, 2005), supported by an excess of Na over Cl (Fig. S9) compared to the opposite in rain water (Appelo and Postma, 2005). Moreover, the release of Na could be increased by the dissolution of Ca-bearing silicates: since they dissolve faster than Na-bearing silicates (Goldich, 1938), the increase in Ca could favor the release of Na via cation exchange. A positive correlation between Na and NH_4 was also found by Norrman et al. (2015) for reducing groundwaters hosted by deep Pleistocene aquifers in Vietnam, whereas other works (Daughney et al., 2010; Morgenstern and Daughney, 2012) pointed out that increasing Na in deep aquifers can be related to progressively older groundwater.

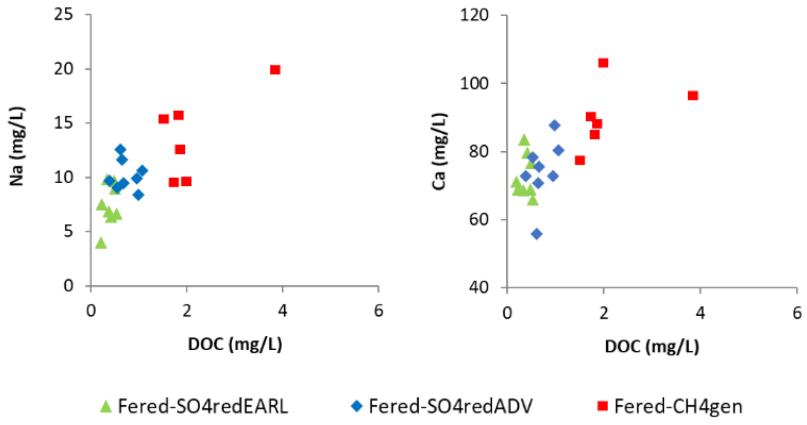

Fig. S8. Scatter plots of DOC vs Na and Ca. Fered-SO4redEARL: groundwaters under Fe-oxide reduction and early-stage sulfate reduction; Fered-SO4redADV: groundwaters under Fe-oxide reduction and advanced-stage sulfate reduction; Fered-CH4gen: groundwaters under Fe-oxide reduction and methanogenesis.

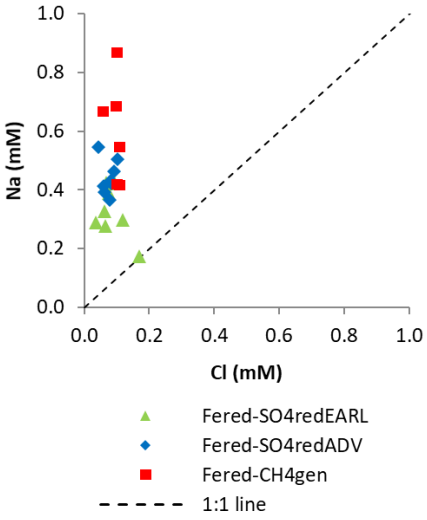

Fig. S9. Scatter plots of Na vs Cl. Fered-SO4redEARL: groundwaters under Fe-oxide reduction and early-stage sulfate reduction; Fered-SO4redADV: groundwaters under Fe-oxide reduction and advanced-stage sulfate reduction; Fered-CH4gen: groundwaters under Fe-oxide reduction and methanogenesis.

Section S6. Mineral equilibria

Speciation and calculation of SI revealed that groundwaters are slightly supersaturated or near dissolution/precipitation equilibrium with respect to carbonates; more specifically, average SI were 0.98 for dolomite ($MgCa(CO_3)_2$), 0.76 for calcite ($CaCO_3$), 0.61 for aragonite ($CaCO_3$), 0.38 for siderite ($FeCO_3$) and 0.06 for rhodochrosite ($MnCO_3$). The equilibrium diagrams for dissolution/precipitation of calcite and aragonite, dolomite, rhodochrosite and siderite are shown in Fig. S10. In addition, Fig. S10 shows the equilibrium plot for vivianite ($Fe_3(PO_4)_2$:$8H_2O$), that had an average SI of -1.18, and a scatter plot for the SI of siderite vs DOC. For calcite and dolomite, the different slope between the equilibrium line and the alignment of measured data indicates that dissolved Ca and Mg are not controlled by dissolution/precipitation equilibrium of their corresponding carbonates. Conversely, the plot for rhodochrosite shows that points are well aligned along the equilibrium line suggesting that rhodochrosite equilibrium can have a key role in controlling dissolved carbonate and manganese concentrations in the system. For siderite, the picture is less clear, while some points (i.e. those under Fe-oxide reduction and early-stage sulfate reduction) seem aligned with a slope similar to that of the equilibrium line and the remaining points do not. This can indicate that other processes, in addition to siderite precipitation, are controlling dissolved carbonates and iron in the system, i.e. rhodochrosite and FeS precipitation/dissolution. Our guess is that siderite is precipitating both under sulfate reduction and methanogenesis, reaching higher SI under methanogenesis due to a) the ceased decrease of Fe concentrations accompanying FeS precipitation and b) the stronger precipitation inhibition exerted by higher DOC concentrations (Berner et al., 1978). Vivianite precipitation does not seem to be part of the processes controlling dissolved Fe, since the equilibrium diagram shows an undersaturation for Fe-oxide and sulfate reducing groundwaters and no clear alignment with the equilibrium line's slope for groundwaters characterized by Fe-oxide reduction and methanogenesis.

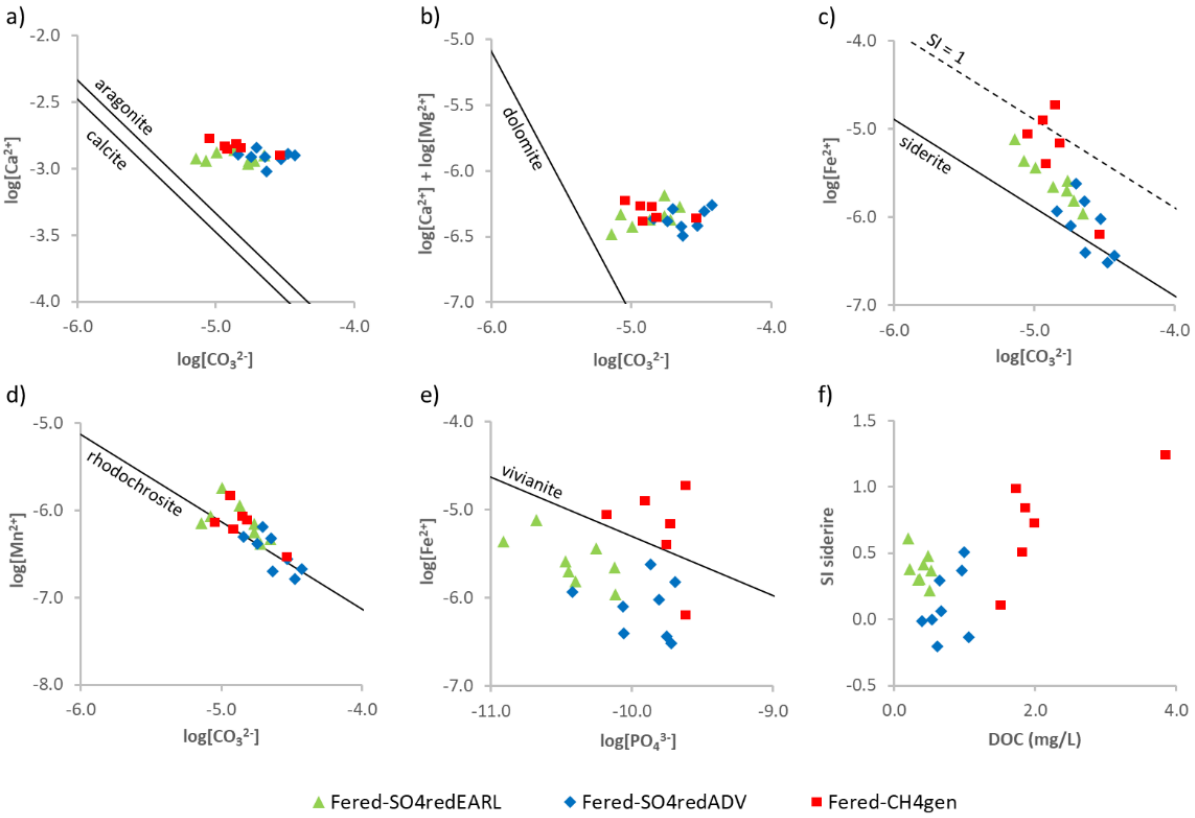

Fig. S10. Chemical equilibrium diagram for dissolution/precipitation of a) calcite and aragonite, b) dolomite, c) siderite, d) rhodochrosite, e) vivianite and f) scatter plot of SI siderite vs DOC; solid lines are equilibrium lines. Fered-SO4redEARL: groundwaters under Fe-oxide reduction and early-stage sulfate reduction; Fered-SO4redADV: groundwaters under Fe-oxide reduction and advanced-stage sulfate reduction; Fered-CH4gen: groundwaters under Fe-oxide reduction and methanogenesis.

References

Appelo, C.A.J., Postma, D., 2005. Geochemistry, Groundwater and Pollution, second. ed. Balkema Publishers, Leiden.

Ball, J.W., Nordstrom, D.K., 1991. User's manual for WATEQ4F, with revised thermodynamic data base and text cases for calculating speciation of major, trace, and redox elements in natural waters. U.S. Geological Survey Open-File Report 91–183. https://doi.org/10.3133/ofr91183

Berner, R.A., Westrich, J.T., Graber, R., Smith, J., Martens, C.S., 1978. Inhibition of aragonite precipitation from supersaturated seawater; a laboratory and field study. Am. J. Sci. 278, 816–837. https://doi.org/10.2475/ajs.278.6.816

Capasso, G., Inguaggiato, S., 1998. A simple method for the determination of dissolved gases in natural waters. An application to thermal waters from Vulcano Island. Appl. Geochem. 13, 631–642. https://doi.org/10.1016/S0883-2927(97)00109-1

Chapelle, F.H., McMahon, P.B., Dubrovsky, N.M., Fujii, R.F., Oaksford, E.T., Vroblesky, D.A., 1995. Deducing the Distribution of Terminal Electron-Accepting Processes in Hydrologically Diverse Groundwater Systems. Water Resour. Res. 31, 359–371. https://doi.org/10.1029/94WR02525

Daughney, C.J., Morgenstern, U., van der Raaij, R., Reeves, R.R., 2010. Discriminant analysis for estimation of groundwater age from hydrochemistry and well construction: application to New Zealand aquifers. Hydrogeol. J. 18, 417–428. https://doi.org/10.1007/s10040-009-0479-2

Esmeijer-Liu, A.J., Kürschner, W.M., Lotter, A.F., Verhoeven, J.T.A., Goslar, T., 2012. Stable Carbon and Nitrogen Isotopes in a Peat Profile Are Influenced by Early Stage Diagenesis and Changes in Atmospheric CO2 and N Deposition. Water, Air, Soil Pollut. 223, 2007–2022. https://doi.org/10.1007/s11270-011-1001-8

Goldich, S.S., 1938. A Study in Rock-Weathering. J. Geol. 46, 17–58. https://doi.org/10.1086/624619

Kendall, C., 1998. Tracing Nitrogen Sources and Cycling in Catchments. Isot. Tracers Catchment Hydrol. 519–576. https://doi.org/10.1016/B978-0-444-81546-0.50023-9

Kendall, C., Aravena, R., 2000. Nitrate Isotopes in Groundwater Systems, in: Cook, P.G., Herczeg, A.L. (Eds.), Environmental Tracers in Subsurface Hydrology. Springer US, Boston, MA, pp. 261–297. https://doi.org/10.1007/978-1-4615-4557-6_9

Kirk, M.F., Holm, T.R., Park, J., Jin, Q., Sanford, R.A., Fouke, B.W., Bethke, C.M., 2004. Bacterial sulfate reduction limits natural arsenic contamination in groundwater. Geology 32, 953–956. https://doi.org/10.1130/G20842.1

Regione Lombardia, 2019. Lombardy Region WebGIS. http://www.geoportale.regione.lombardia.it (accessed 3.10.19).

Morgenstern, U., Daughney, C.J., 2012. Groundwater age for identification of baseline groundwater quality and impacts of land-use intensification – The National Groundwater Monitoring Programme of New Zealand. J. Hydrol. 456–457, 79–93. https://doi.org/10.1016/J.JHYDROL.2012.06.010

Nikolenko, O., Jurado, A., Borges, A. V, Knöller, K., Brouyère, S., 2018. Isotopic composition of nitrogen species in groundwater under agricultural areas: A review. Sci. Total Environ. 621, 1415–1432. https://doi.org/10.1016/j.scitotenv.2017.10.086

Norrman, J., Sparrenbom, C.J., Berg, M., Dang, D.N., Jacks, G., Harms-Ringdahl, P., Pham, Q.N., Rosqvist,

H., 2015. Tracing sources of ammonium in reducing groundwater in a well field in Hanoi (Vietnam) by means of stable nitrogen isotope (δ15N) values. Appl. Geochem. 61, 248–258. https://doi.org/10.1016/J.APGEOCHEM.2015.06.009

Rotiroti, M., Bonomi, T., Sacchi, E., McArthur, J.M., Stefania, G.A., Zanotti, C., Taviani, S., Patelli, M., Nava, V., Soler, V., Fumagalli, L., Leoni, B., 2019. The effects of irrigation on groundwater quality and quantity in a human-modified hydro-system: The Oglio River basin, Po Plain, northern Italy. Sci. Total Environ. 672, 342–356. https://doi.org/10.1016/J.SCITOTENV.2019.03.427

Rotiroti, M., McArthur, J., Fumagalli, L., Stefania, G.A., Sacchi, E., Bonomi, T., 2017. Pollutant sources in an arsenic-affected multilayer aquifer in the Po Plain of Italy: Implications for drinking-water supply. Sci. Total Environ. 578. https://doi.org/10.1016/j.scitotenv.2016.10.215

Velinsky, D.J., Pennock, J.., Sharp, J.., Cifuentes, L.., Fogel, M.L., 1989. Determination of the isotopic composition of ammonium-nitrogen at the natural abundance level from estuarine waters. Mar. Chem. 26, 351–361. https://doi.org/10.1016/0304-4203(89)90040-6